Sundarban: A Review of Evolution & Geomorphology

Sunando Bandyopadhyay

Department of Geography, University of Calcutta, Kolkata - 700019

Email: sunando@live.com

Structure of the Article

Sundarban: A Review of Evolution & Geomorphology

Sunando Bandyopadhyay

Department of Geography, University of Calcutta Kolkata 700019
E-mail: sunando@live.com

ABSTRACT: The Sundarban mangrove wetlands occupy the western part of the lower Ganga–Brahmaputra delta (GBD), Bangladesh and India. Formation of the Bengal basin, the cradle of the GBD, started in the Jurassic with initiation of rifting of the Pangaea and completed by the Miocene with docking of eastern India with the Burma platelet. Sedimentation of the basin started almost contemporaneous to rifting and occurred in the three geotectonic provinces of continental shelf, deeper basin areas, and Chittagong-Tripura Fold Belt. The GBD originated with the opening of the Rajmahal-Garo gap in the Plio-Pleistocene. It acquired its present form during the late Holocene after the sea level neared its present position. The Holocene history of the delta was characterised by fluctuations in monsoon-related sediment discharge, land- and seaward migrations of depocentres and at least five switching in the course of the Brahmaputra. Four Holocene sedimentary facies, up to the depth of ~90 m, can be distinguished in the delta proper. The coastal region of the delta is not older than 5~2.5 ka and was developed by formation of four overlapping and eastward-younging deltaic lobes. Accreted by biotidal processes and shaped by marine and atmospheric agencies, the intensity of which varies over space and time, the Sundarban is now fluvially abandoned. Landforms of the region can be classified into the broad morphotypes of beach, dune, estuary bank, swamps, and reclaimed plains apart from process- and feature-based subtypes. Although erosion of the estuary margins and seaface—up to 40 m a^{-1}—is continuing for many decades in Sundarban, interior channels, especially in the west, are getting silted up. These changes can be ascribed to sediment reworking in a flood-tide dominated environment that is greatly intervened by reclamation efforts, initiated in 1770. Research during the past two decades has brought out a number of physical trends that can be utilised to formulate a holistic plan that would address the key issues of the Sundarban. Estimates of relative mean sea level rise for the region range between 1.2 and 6.3 mm a^{-1}. However, rate of high water level rise, at 10–17 mm a^{-1}, is assessed to be much higher than this in some sections. On the other hand, in forested stretches of Sundarban, vertical accretion rate from tidal inundation is ~10 mm a^{-1}, which can increase to 180 mm a^{-1} in sediment-starved reclaimed regions, if exposed to tidal spill. This opens up the possibility of elevation recovery in the reclaimed Sundarban through phased removal of embankments. Future planning for the region must accept the transformations that are brought into the system by the humans and strike a balance between the requirements of the nature and the needs of the people.

1. INTRODUCTION

Located at the northern apex of the Bay of Bengal, the Ganga–Brahmaputra delta (GBD) is the world's largest both in terms of land area (15,000 km^2) and yearly discharge of sediments (~10^9 t a^{-1}). The delta is contributed by a combined catchment area of 1.6×10^6 km^2, drained by many small to medium sized peripheral streams that emanate from the surrounding uplands apart from the Ganga and the Brahmaputra.

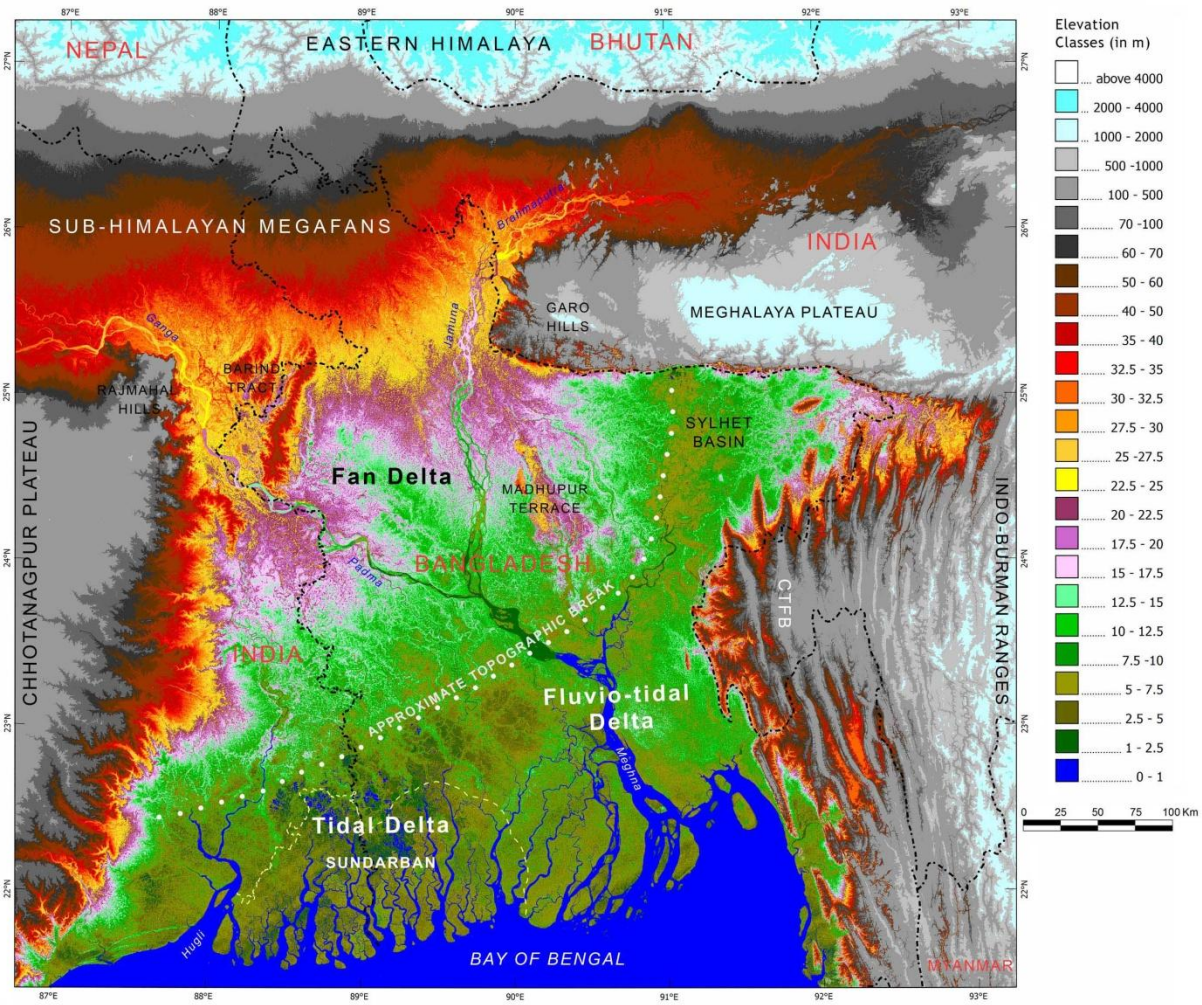

Figure 1: Physiographic setting of the Ganga Brahmaputra delta. The plateaus and other highlands generally occupy the zones above 60 m. Elevation of the alluvial fans, palaeodeltas and Pleistocene terraces approximately range between 25 and 60 m. Areas lower than this form the delta proper. The elevations of the delta roughly decrease from NW to SE. Gradient- and process-based divisions of the delta adapted from Wilson and Goodbred (2015). Limit of the Sundarban region shown in yellow dashed line; see Fig. 9 for details of this boundary. CTFB stands for Chittagong–Tripura Fold Belt. *Source*: Elevation model prepared from 90-m Shuttle Radar Topography Mission data of 2000

The GBD, of which Sundarban forms the coastal part, is bordered by highlands on all three sides barring a 125-km-wide passage that links the region to its northern provenance. This is known as the Rajmahal–Garo Gap (RGG), a worn-down saddle of the Indian craton between the Rajmahal and the Garo hills (Fig. 1). Besides the RGG, the northern and eastern boundaries of the delta are defined by the crystallines of the Meghalaya plateau, the Rajmahal hills and the Chhotanagpur plateau, all of which were parts of the Gondwanaland up to the Jurassic. The eastern boundary of the delta is delineated by the Neogene sedimentaries of Chittagong–Tripura Fold Belt (CTFB).

The subaerial and subaqueous parts of the GBD can be seen as integral parts of the Bengal Depositional System that stretches from south of the Himalaya to the distal edge of the Bay of Bengal (Curray, 2014). Its deltaic components include • a higher-gradient fan delta in the north, characterised by vertically and laterally migrating sand-dominated braidbelts; • a lower-gradient fluvio-tidal section in the southeast which is building into the sea with comparatively stable channels; and • a fluvially abandoned tidal section in the southwest that is accreting vertically but also declining irreversibly in certain sections (Wilson and Goodbred, 2015).

The current orientation of the Ganga–Padma–Lower Meghna river diagonally divides the GBD into two parts. The southwestern portion, along with southern coastline of the delta between the Hugli and the Baleswar estuaries, is primarily contributed by the distributaries of the Ganga system—active or dissipated. Its 200-km littoral stretch constitutes about 47% of the GBD coastline and harbours the largest contiguous mangrove forests of the world—the Sundarban.

This article first reviews the evolution of the Sundarban region as a part of the Bengal basin and the GBD. It then discusses the main natural and anthropogenic forcings working on the area and how the region is responding to them.

2. EVOLUTION OF THE DELTA

The cradle of the GBD is the Bengal basin — a structural depression filled up by the rivers during the last ~150 Ma. The evolution of the basin was controlled by a series of tectonic and sedimentation phases related to plate movement, palaeoclimate and eustasy.

2.1 Cretaceous-Tertiary evolution

India detached from the eastern Gondwanaland and started drifting northwards during Early–Late Cretaceous, c. 133–93 Ma BP (Fig. 2A) (Lawver *et al*., 1985). The northern and western parts of the Bengal basin took shape on the continental shelf that skirted this newly formed subcontinent (Fig. 2B). Deltas began to accrete on the shelf and continued to prograde till they merged with the materials brought down by the Ganga and the Brahmaputra in the Quaternary (Niyogi, 1975; Agarwal and Mitra, 1991). These palaeodeltas now resemble a coalescing fan system of the western tributaries of the Bhagirathi–Hugli river. About 50 Ma later, in Early Eocene, India collided with the Tibetan mainland and the rise of the Himalaya was initiated (Curray et al., 1982; Chen et al., 1993). At about 44 Ma BP (Mid Eocene), the Indian plate added a counter-clockwise orientation to the post-collision movement as a sequel to the opening of the Arabian sea (Fowler, 1990). Due to the shape of the northeastern edge of the Indian continent and this rotational movement, the subduction in the Indo-Burmese sector progressed obliquely (Fig. 2C) and the remnant ocean basin between eastern India and Burma was subjected to a 'zipper-like' closure from north to south (Biswas and Agrawal, 1992). Sediments from Burma are first detected in the Bengal basin in the Early Miocene (Steckler *et al.*, 2008). This signals acquiring of a continental boundary to its east. As the oceanic part of the Indian plate continued to slide under the Burma platelet, the eastern sector of the Bengal basin changed to a subduction-related mountain building area and evolved into the Chittagong–Tripura Fold Belt (CTFB).

In this way, the Bengal basin traversed some 70 degrees of latitude (~7,700 km) from its original pre-drift locality. It witnessed transformation from an open continental shelf-slope setting of a drifting continent into a miogeosynclinal foredeep at the foot of a young folded mountain that now defines its eastern boundary. Earthquakes continue to originate in the eastern section of the basin since the historical times, indicating tectonic adjustments (Nandy, 1986; Steckler *et al.*, 2008). The channel avulsion patterns of eastern portion of the delta are largely steered by tectonics (Reitz *et al.*, 2015). As Morgan and McIntire (1959:335) observed, 'active, Recent faults of the magnitude present in the Bengal Basin are unusual'.

Three tectonic provinces are distinguishable in the Bengal basin (Alam, *et al*., 2003): (1) the shelf region, underlain by continental crust; (2) the deeper basin region, underlain by oceanic crust and (3) the folded sediments of the arc-trench accretionary prism — the CTFB. The GBD and the Sundarban essentially rest on the first two of these. The principal features and events pertaining to the basin are summarised in Table 1 and Fig. 3A and 3B.

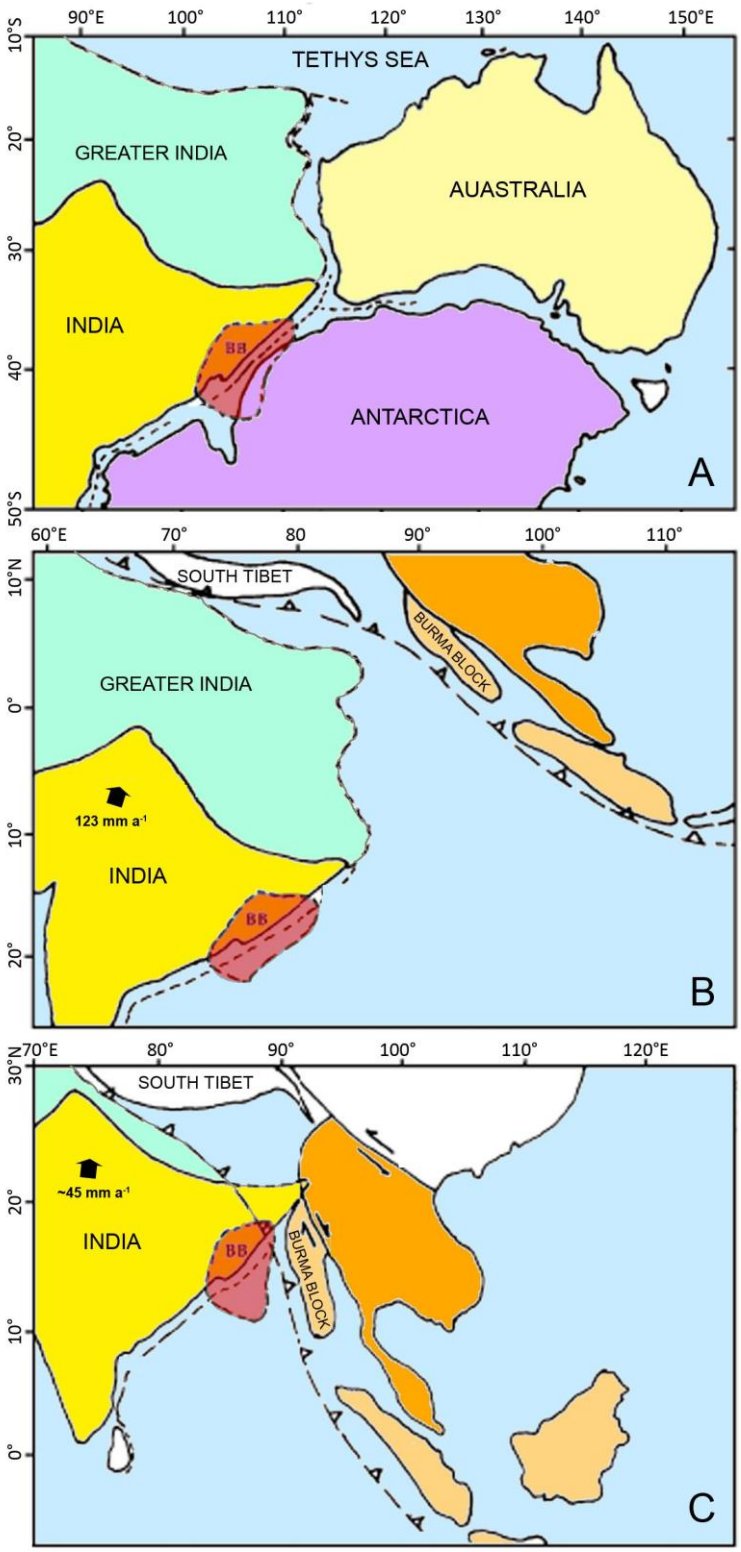

Figure 2: Palaeographic reconstructions showing the position of the Bengal basin region (**A**) at the break-up of the Gondwanaland in Early Cretaceous; (**B**) in a continental shelf-slope setting in the northward drifting island-continent of India in Mid-Palaeocene and (**C**) in Early Miocene prior to acquiring its eastern boundary in form of the Indo-Burman and associated ranges. 'BB' stands for the Bengal basin region, shown in red. Blue indicates oceans and other colours represent continents. Undifferentiated areas are shown in white. The area termed Greater India was consumed in the subduction process and crustal shortening during formation of the Himalaya. *Source*: based on Alam et al.'s (2003) adaptation of Lee and Lawver (1995). Drift velocities from Lee and Lawver (1995)

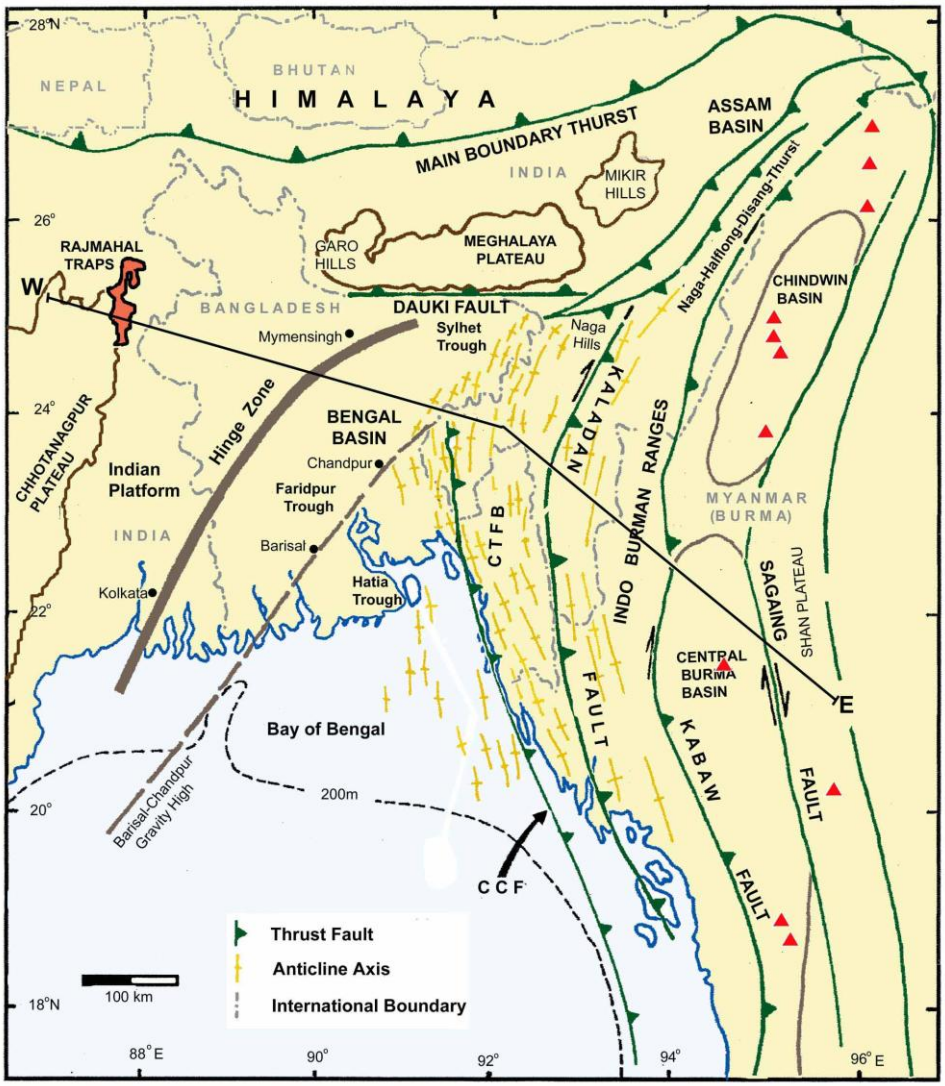

Figure 3A: The Bengal basin and its surroundings featuring the chief tectonic elements. The Hinge Zone marks the outer edge of the continental shelf of the Indian craton and initiation of southeastward attenuation of the continental crust (Tectonic Province-1). The Barisal-Chandpur Gravity High marks the transition from continental to oceanic crust at the base of the Bengal basin (Tectonic Province-2). CTFB and CCF stand for Chittagong–Tripura Fold Belt (Tectonic Province-3) and Chittagong–Cox's Bazar Fault respectively. CCF is the approximate linearity along which the Indian Plate is now subducting beneath the Burma platelet. Red triangles denote Tertiary volcanic centres, formed out of the ongoing subduction. *Source*: after Alam *et al.* (2003). Some Elements are incorporated from Nandy (2001) and Gani and Alam (2003)

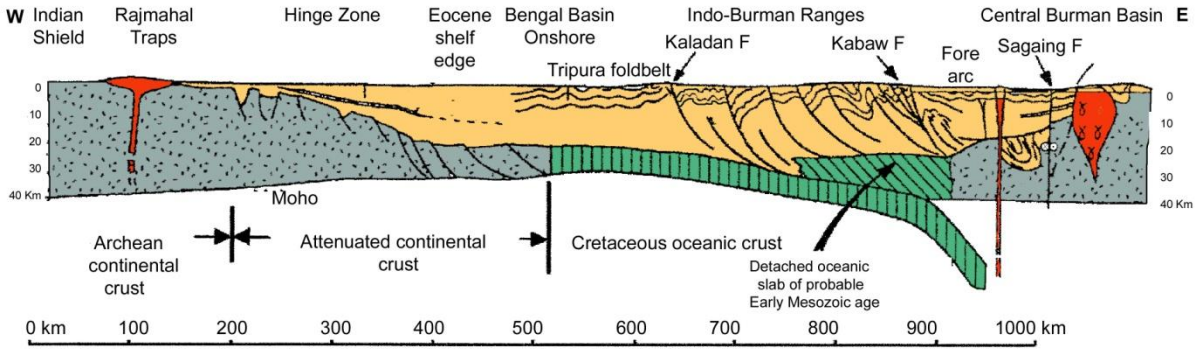

Figure 3B: West–East section across the Bengal basin showing major tectonic and crustal features. Volcanics are shown in red. See Fig. 3A for location of the section line. *Source*: after Alam *et al.* (2003)

Table 1: Sedimentation phases in Bengal basin (based on Alam *et al*., 2003)

Phases	Time	Tectonic stage / event	Sedimentation pattern
V	Mid Pliocene – Quaternary	Continued uplift of the Meghalaya plateau. Subsidence of the Sylhet basin made it a part of Tectonic Province-2.	Sedimentation in Provinces-1 & 2 affected by glacio-eustatic oscillations superposed on general regression. The Hatiya trough of Province-2, grading into the deep sea Bengal fan, emerged as the presently active depocentre.
IV	Early Miocene – Mid Pliocene	Late (hard) collision of India and Asia. Start of uplift of the Meghalaya plateau (Early Miocene); subsidence and separation of the Sylhet trough from Province-1.	Early Miocene uplift of the eastern Himalaya increased sediment influx from the northeast in Provinces-2 and 3. Sediments from Burma started reaching the basin from Early Miocene (Steckler *et al.*, 2008).
III	Mid-Eocene – Early Miocene	Early (soft) collision of India and Asia; Westward shift of subduction zone beneath the Burma platelet CTFB (Late Oligocene).	Basin-wide regression by Oligocene and deposition of clastics. Provinces-2 and 3 accreted as active depocentres. Folding of Tectonic Province-3 sediments started from Late Oligocene. The soft-collision had little effect on Bengal basin sedimentation.
II	Cretaceous – Mid-Eocene	Opening of the Indian ocean and northward drift of the Indian continent.	Marine transgression in Provinces-1 and 2 up to the Eocene: deposition of shales and limestones (partly derived from coral reefs).
I	Permo-Carboniferous – Early Cretaceous	Rifting of India within the Gondwanaland.	Sedimentation in Tectonic Province-1 with occurrence of coal, topped by Rajmahal traps and trapwash.

2.2 Quaternary evolution

Accretion of the modern GBD was initiated with the opening of the RGG in the Pliocene (Alam, 1989; Khan, 1991) or Pleistocene (Auden, 1949). At the inception of the Quaternary, while the main GBD was gradually being accreted by the Ganga and the Brahmaputra from north and along the central section through the RGG, smaller peripheral streams were simultaneously contributing sediments along the basin boundary. Despite the fact that the depth of the Mio-Pliocene surface does not vary appreciably along the same latitude between the eastern and western edges of the Bengal basin (Khan, 1991), deltaic progradation had probably been more prominent in the western basin margin, compared to the east owing to the comparatively larger size of the rivers.

The Pleistocene is marked for fluctuations in global temperature that brought four cool glacial stages and the intervening warm interglacials. Intrinsically linked to the global hydrological cycle, the cool (warm) epochs caused worldwide fall (rise) in the secular mean sea level. The latest glaciation ended about 15~12 ka BP, establishing the onset of the Holocene. The GBD, like all modern deltas of the world, was primarily shaped during this period. Therefore, events of the Holocene constitute a crucial part in its evolutionary history.

2.2.1 Holocene Sea-Level curve

The Holocene secular man sea level (MSL)/time curves provided by different workers connote a quick rise at ~10 mm a^{-1} between 15 ka and 6 ka, which slowed down to 0.5 & 0.1–0.2 mm a^{-1} during the last 6 ka & 3 ka respectively (Pugh, 2004). This means that the MSL had almost reached its present position some 6 ka BP after which it is rising slowly. The fast rate of MSL rise during the early Holocene caused worldwide inundation of low-lying coastal areas. Estimations of these rates for the GBD are summarised in Table 2 and Fig. 4.

Table 2: Selected estimates of Holocene sea level and rates of rise in the GBD

Source	Area	Early Holocene	Late Holocene	Method / Remarks
Banerjee and Sen, (1987), Sen and Banerjee (1990)	Western lower GBD (India)	–7 m of present sea level (PSL) at 7 ka BP	0 PSL at 5 ka BP	Dating of palyno-plankton stratigraphy and proxydata on bio-remain assemblages
Hait *et al.* (1996)	Western lower GBD (India)	8.8 mm a^{-1} (9.8–5 ka BP)	0.7 mm a^{-1} (6.2–4.7 ka)	Dating of five core samples along a traverse
Umitsu (1987)	Eastern GBD (Bangladesh)	–47 m PSL at 12.3 ka BP, increased thereafter at 5.5 mm a^{-1}	–15 m PSL at 6.4 ka BP increased thereafter at 2.3 mm a^{-1}	Dating of woods, shells and other organic samples from different levels of Holocene stratigraphy
Goodbred and Kuehl (2000a)	Eastern GBD (Bangladesh)	60~70 (22~35) m lower than the PSL at 10 (7) ka BP	17~29 m lower than the PSL at 6 ka BP	Proxydata and sample dating. Values adjusted to the delta's subsidence rates
Islam (2001)	Eastern GBD (Bangladesh)	—	1.07 mm a^{-1}, with a maximum of 3.65 mm a^{-1} (6.3–5.9 ka BP) and a minimum of 0.81 mm a^{-1} (4.4–2.3 ka BP)	Subsidence-corrected pollen and diatom dating of cores samples from Dhaka and Khulna

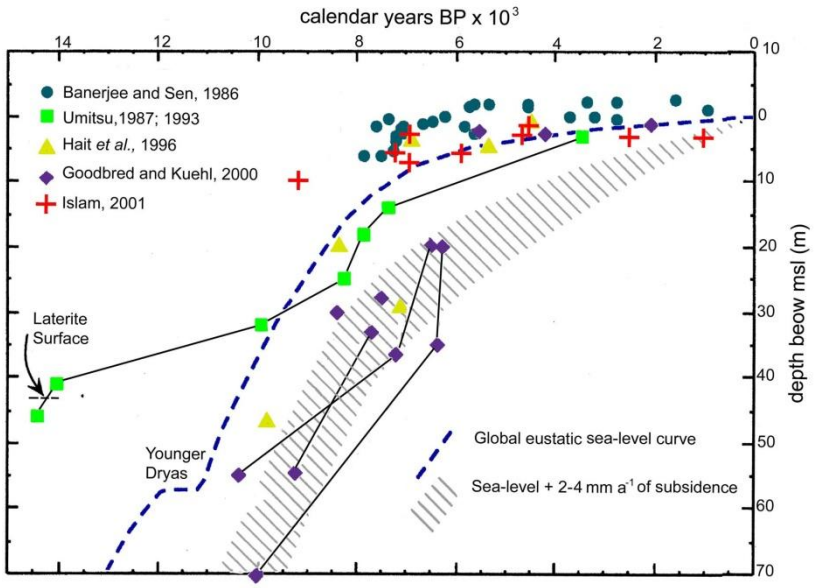

Figure 4: Plot of ^{14}C dates against depth of organic samples from the Ganga-Brahmaputra delta. Subsidence and tectonic instability is a major concern for accuracy and standardisation of results. Plots joined by a line come from same borehole. The Younger Dryas represents a brief cold period between c. 12.7 and 11.5 ka BP. *Source*: after Goodbred and Kuehl (2000a) with data of Islam (2001) incorporated

It is important to note that although evidence of land subsidence is common in the Sundarban (Blanford, 1864; Gastrell, 1868:26–28; Fawcus, 1927; Haque and Alam, 1997), some of the above studies did not consider this appreciably. Compared to other large deltas, the general dominance of silts and sands over clays significantly prevents autocompaction in the GBD sediments (Goodbred and Kuehl, 2000a, Kuehl, *et al.*, 2005). Tectonics is regionally capable of initiating channel avulsion in GBD (Reitz *et al.*, 2015) and is also a cause of the 2–4 mm a^{-1} subsidence estimated for its central and coastal parts (Goodbred and Kuehl, 2000a). For the western Sundarban, Stanley and Hait (2000) estimated subsidence up to 5 mm a^{-1} against sediment accumulation of up to 7 mm a^{-1}. For shorter time span, Hanebuth *et al.* (2013) dated mangrove roots and archaeological remains from the Khulna Sundarban and estimated subsidence of 5.7 mm a^{-1} and 4.1 ± 1.1 mm a^{-1} for the last 360 a and 300 a, respectively. This

may be compared with the available subsidence rate of ~3 mm a^{-1} from short-term GPS measurements near Patuakhali at the coastal delta, east of the Sundarban (Reitz *et al.*, 2015).

2.2.2 Holocene evolution

The ~8,500 km^3 Holocene sequence in the Bengal basin varies from c. 15 m over the eastern platform (Tectonic Province-1) to some 90 m in the deeper basin areas (Tectonic Province-2) (Allison, *et al.*, 2003; Goodbred *et al.*, 2014). The broad framework of evolution of the GBD is outlined in the following sections based mainly on Goodbred and Kuehl (2000a) and Goodbred (2003). Table 3, Fig. 5 and Fig. 6 provide summaries of the changing scenarios.

THE LOWSTAND SCENARIO (24–18 ka BP): The glacial lowstand was at its maximum (Fig. 5A). Exposed laterised uplands and incised valleys, often containing lag gravels, were widespread. River discharges were low, probably insignificant, compared to the present. MSL was some 100 m lower than the present. About 80–100-km wide stretch of continental shelf became exposed off the GBD to subaerial processes (Niyogi, 1972; Alam, 1989), and may have extended up to the shelf break (Cochran, 1990). Existence of cut and fill channels on the shelf area supports this observation (Saxena *et al.*, 1982). At this time, salinity of the northern Bay of Bengal was at least 4‰ higher than the present due to absence of freshwater discharge (Cullen, 1981).

ONSET OF WARMING (15 ka BP): The upper part of the submarine Bengal fan started receiving fresh sediment input, indicating onset of climatic warming and strengthening of the summer monsoon and increase in discharge levels. The accumulation rate at the submarine Bengal fan off the GBD greatly increased up to about 11 ka BP when the rising MSL submerged large areas of the delta that transferred the depocentre landwards with extensive development of floodplains. Since ~12 ka BP, the valleys incised during the lowstand were started to fill up with sands (Facies-II of Table 2).

DELTA DEVELOPMENT COMMENCED (11.5–10 ka BP): By 11.5 ka BP, intensity of the sothwest monsoon became significantly higher, which shot up sediment discharge at least 2.5-times of their present level. The incised river valleys started to fill-up with sand (Fig. 5B) (Goodbred and Kuehl, 2000b). However, a high rate of sedimentation at the Bengal fan connotes that the incipient GBD was incapable of accommodating a large part of the load it received. A couple of wood fragments and a shell, found below and ~10 m above the low-stand laterite horizon respectively, were dated ~14 ka BP and ~ 9.9 ka BP by Umitsu, 1993 (Fig. 4). This indicates that the delta growth must had started at about 10~11 ka BP. At this time the Bengal fan sedimentation also recorded a sharp decline indicating shift of the depocentre to on-shore localities. The MSL rose to –45 m, submerged a large part of the basin and started to trap sediments that initiated the development of the modern GBD system. In the southern basin, 20–25 m-thick fine Lower Delta Mud facies (Facies-III of Table 2) covered most of the lowstand laterised surfaces (Facies-I) in a near-shore mangrove-dominated depositional environment. In northern parts of the basin, clean Sand sequences (Facies-II), associated with fluvial channels, continued to be deposited in the central valleys.

DELTA DEVELOPMENT DURING RAPID RISE OF SEA LEVEL (11–9/7.5 ka BP): The delta continued to agrade as the huge sediment load of the Ganga–Brahmaputra system largely compensated the rise in the MSL. This scenario, matched in few areas of the world (Kuehl *et al.*, 2005), persisted as the MSL rose to –15 or –10 m at the end of this period at ~10 mm a^{-1}. Continuous subsidence of the Sylhet basin repeatedly altered the hydraulic gradient of the Mymensingh corridor between the Meghalaya plateau and the morphotectonic Madhupur terrace. Filling-up of the basin makes the passage between the Barind and Madhupur terraces—the one currently followed by the Brahmaputra river—comparatively steeper; but only up to the point when subsidence of the Sylhet basin alters it to the Mymensingh passage's favour. Consequently,

the Brahmaputra switched its course at least five times in the Holocene between these two corridors (Goodbred and Kuehl, 2000a; Heroy *et al*., 2003). Deposition of Fine Mud facies in the northeastern Sylhet basin started only after 9 ka BP, indicating that after this time the Brahmaputra was following its western course (Avulsion-I: W⇦E), and discharging its sediments directly into the sea, until ~7.5 ka BP. This, although starved the subsiding Sylhet basin from filling-up, supported the maintenance of shoreline stability of the delta front at the time of rapid rise in MSL.

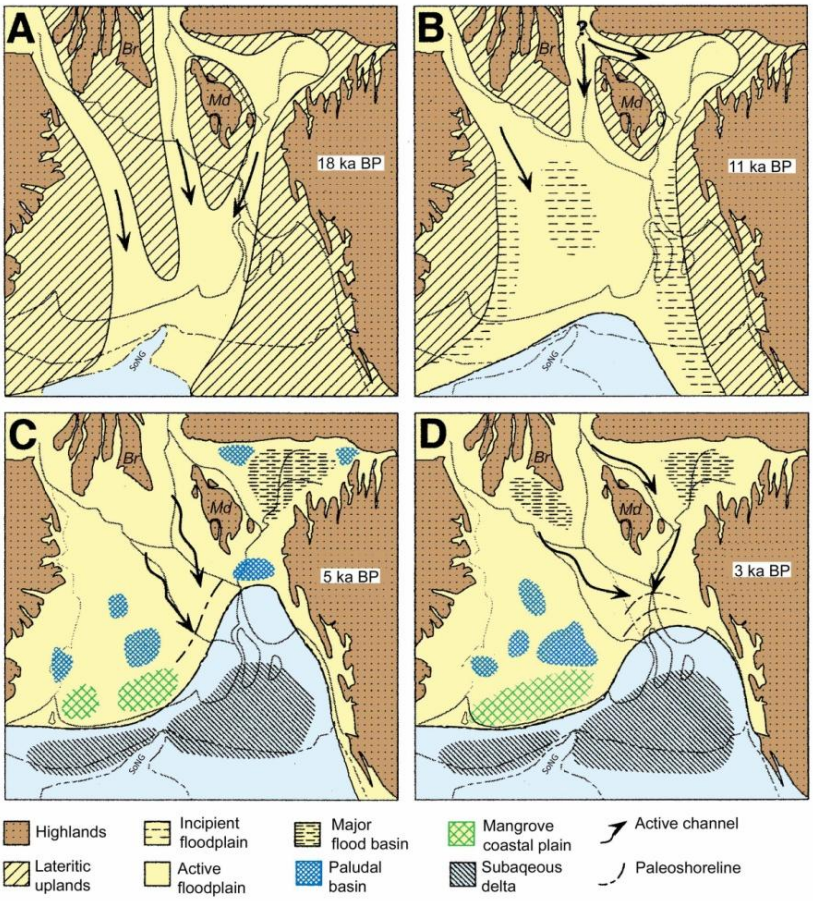

Figure 5: Panels representing principal features of the Late Quaternary evolution of the Ganga-Brahmaputra delta. See text for explanation. *Br*, *Md* and *SNG* stand for the Barind tract, Madhupur terrace and Swatch of No Ground submarine canyon, respectively. Cf: Fig. 6. *Source*: modified after Goodbred and Kuehl (2000a)

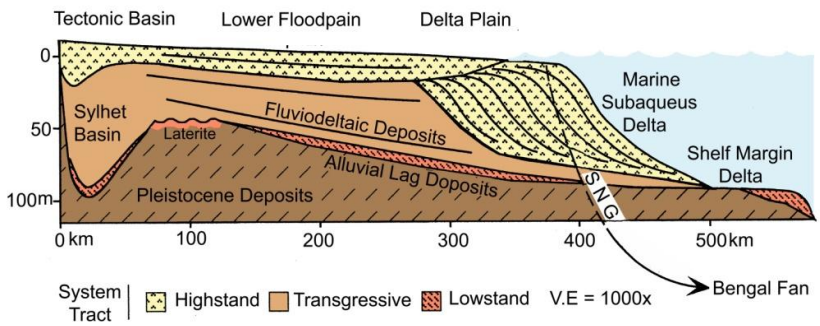

Figure 6: Schematic section showing sequence stratigraphy of the Holocene Ganga–Brahmaputra delta (vertical exaggeration: 1000×). Transgressive facies belong to on-lapping sequences and high-stand regressive facies to off-lapping formations. Other elements of the diagram are explained in the text. SNG stands for Swatch of No Ground submarine canyon that works as a trap of delta sediments and a conduit of sediment transfer to the deep sea Bengal fan. *Source*: from Goodbred and Kuehl (2000a)

Table 3: Summary of stratigraphic facies of the Ganga-Brahmaputra delta (after Goodbred and Kuehl, 2000a)

Facies	Period of Deposition	Distribution	Sedimentology	Colour	Thickness	Depth to top	Interpretation
VI: THIN MUD	c. 5–0 ka BP	Floodplain environments throughout, absent near fluvial channels	Variable soft, muddy sediments with occasional fine sands	Brown to grey-brown	2–7 m	Surface; locally 20–40 m	Abandoned floodplain and overbank deposits
V: SYLHET BASIN MUD	c. 10–0 ka BP	Sylhet basin, also along the Brahmaputra channel	Variable silt-dominated sediments with 0–70% sand and 5–90% clay	Brown-grey to blue grey	60–80 m	3–5 m	Tectonic floodbasin deposits
IV: MUDDY SAND	c. 8–3.5 ka BP	South-central delta	Variable fine sand-dominated sediments with 25–80% muds	Brownish grey	30–35 m (locally 10 m)	4–7 m	Estuarine, distributary-mouth channel deposits
III: LOWER DELTA MUD	c. 12–7.5 ka BP	South-central delta: tidally influenced area	Silt-dominated sediments with 15–35% clay and 0–35% fine sand	Brownish grey	20–25 m (locally 7 m)	16–40 m	Coastal plain and delta front deposits (likely mangrove)
II: SAND	After c. 12 ka BP	Widespread except in central Sylhet basin. Present as basal unit where oxidised facies are absent	Fine, medium, and generally 'fining upward' coarse sands with abundant micas and heavy-minerals	Grey	15–80 m	5–65 m	Alluvial valley and river channel fill
I: OXIDISED	Pre-Holocene	Locally throughout, particularly adjacent to exposed uplands	Generally stiff muds underlain by medium quartzose sands	Yellow-brown to orange	5–10 m	Surface to c. 45 m	Lateritic uplands of lowstand exposure

MAXIMUM HOLOCENE TRANSGRESSION AND DELTA PROGRADATION THEREAFTER (7.5–5 ka BP): The rate of SL rise slowed around 7.5 ka BP and the maximum landward limit of inundation was achieved in the western part of the basin (Fig. 5C). This had brought the delta coast 'in line with an arc that swung across from south of Calcutta almost to Dhaka and then more closely followed the present coast to the southeast' (Alam, 1989:137). The delta transformed from an aggradational (on-lapping, vertically accreting) to progradational (off-lapping, horizontally accreting) system and the main depocentre started to migrate seaward (Goswami and Chakrabarti, 1987; Chakrabarti, 1995). Extensive dispersal of sands started on the coastal plain as the upstream alluvial valleys were topped up. This laid the Muddy Sand deposits onto the mangrove-dominated coastal plains (Facies-IV of Table 3). A muddy submarine delta begun to take shape at about 7.5 ka BP as well and that made GBD a compound entity with clearly defined subaerial and sub-aqueous components. The Muddy Sand deposits (Facies-IV) can be viewed as the topset beds to both the components (Fig. 6). The growth of the delta clinoform continued and the western delta approached its present extent by ~5 ka BP. This also heralded the formation of coastal peat layers and abandonment and eastward migration of the active Ganga distributaries, leading to the formation of the Sundarban area.

Between 7.5 ka and 6 ka BP, the Brahmaputra returned to its eastern course to the Sylhet basin that started to rapidly fill up at > 20 mm a^{-1} (Avulsion-II: W⇨E). This was also the time when maximum Holocene transgression was achieved in the eastern delta, some 1 to 2 ka after the western part. Between 6 ka and 5 ka BP, as the Sylhet basin sediments indicate, the Brahmaputra switched its course again and returned west (Avulsion-III: W⇦E). With this change, the river probably joined the Ganga, now migrated eastward, for the first time in Holocene (at ~5 ka). By mid-Holocene, the antecedent lowstand valleys of the major streams like the Ganga, the Brahmaputra and the Meghna were mostly filled-up and the rivers started to avulse and migrate freely across the floodplains much like today (Goodbred *et al.*, 2014).

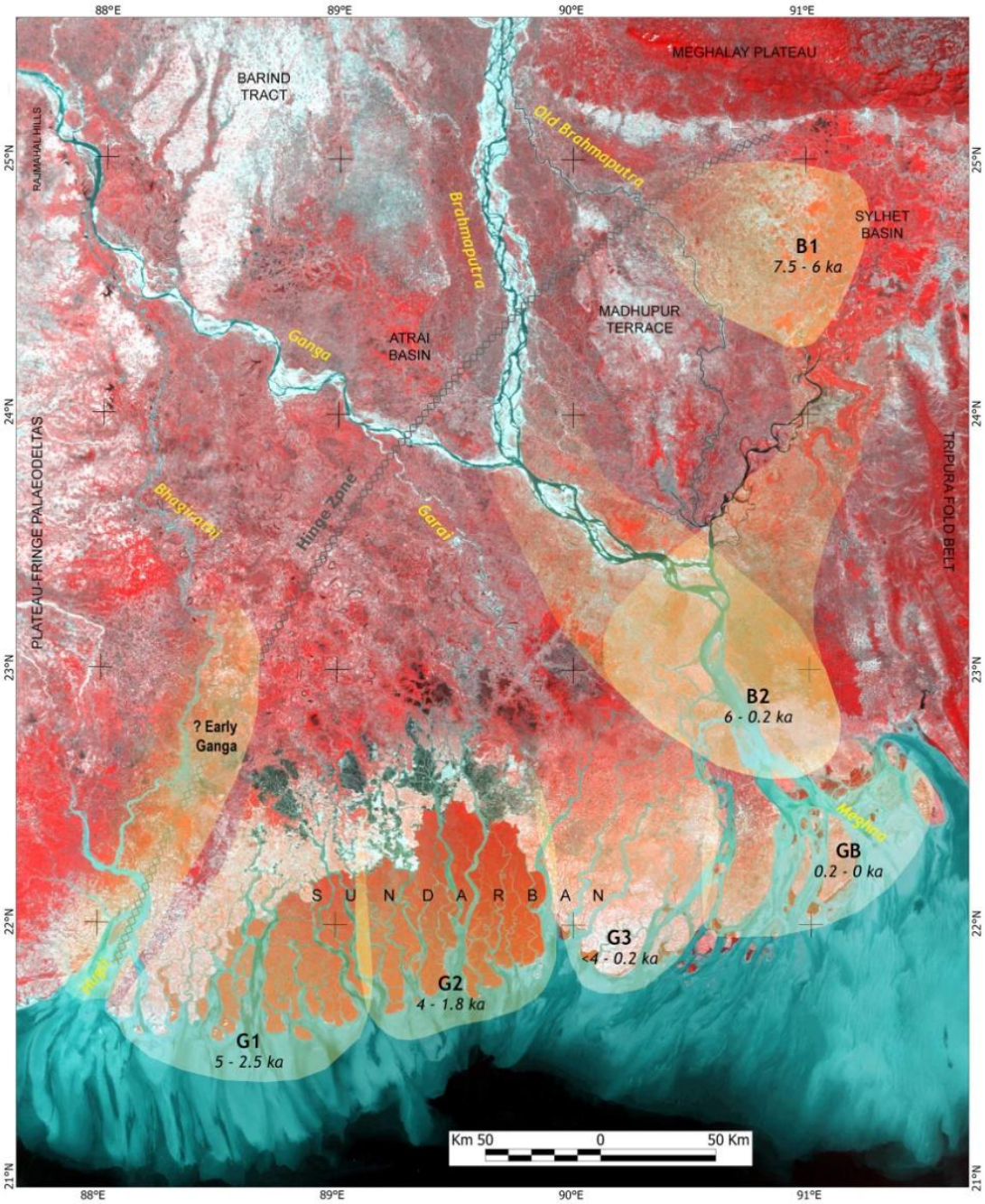

Figure 7: Phases of late Holocene growth of the delta, associated with progressive shifts of the Ganga (G1, G2 & G3), Brahmaputra (B2 & B2) and combined Ganga–Brahmaputra (GB-1) discharges as suggested by Allison *et al*. (2003). Major morphological features of the GBD are also shown. The Barind tract and Madhupur terrace are uplifted blocks with remnant Pleistocene surfaces that separate the delta into different compartments and hinder free swinging of rivers across the delta. Morphostratigraphically equivalent formations are seen in the palaeodeltaic surfaces bordering the Chhotanagpur plateau. The hinge zone is a flexure of the subsurface continental shelf to the deeper basin areas. Reddish tinge in the coastal region denotes the Sundarban mangroves. See Fig. 1 for altitudinal reference. False Colour Composite prepared from IRS-1D WiFS data of 3 March 1998. *Source*: from Bandyopadhyay (2007)

EASTWARD YOUNGING OF THE COASTAL DELTA (5–0 ka BP): During this time, the delta development shifted its focus mainly towards the east and the eastern coastline gradually swung southward to its present position. At least another avulsion of the Brahmaputra occurred (Avulsion-IV: W⇨E) after which it gradually abandoned its course through the Sylhet basin between 1810 and 1850 (Fergusson, 1863:334; Hirst, 1915:180) and established

into its modern channel (Avulsion-V: W⇦E). In fact, the paths of the Ganga and the Brahmaputra swung across the central part of the delta for the major part of the Holocene. In certain localities, provenance of the sediments brought down by the rivers indicated two to six switchings between the two rivers (Heroy *et al.*, 2003).

In the coastal GBD, clay mineralogy, elemental traces and ^{14}C chronology indicate a younging trend towards the east in four overlapping phases (Allison *et al.*, 2003). The westernmost part of the coastal delta—comprising whole of the 24 Parganas Sundarban—was accreted during 5–2.5 ka BP (lobe G1 of Fig. 7). This observation is consistent with ^{14}C dating of samples from Namkhana (+2.25 MSL) and Gangasagar (0.9 m bgl) that indicated dates of 3,170±70 a (Gupta, 1981) and 2,900±20 a (Chakrabarti, 1991) respectively. It also agrees with suggestions that the evolution of the Sundarban part of the GBD commenced after 5 ka BP (Umitsu, 1987) or during 4.5–3.2 ka BP (Banerjee and Sen, 1987). The delta growth then shifted east in phases that lasted 4–1.8 ka BP, <4–0.2 ka BP and 0.2–0 ka BP, corresponding to G2, G3 and GB of Fig. 7, respectively. Among these, only the last phase, which represents modern discharge from the Meghna estuary, contains any significant share of the Brahmaputra sediments (Allison *et al.*, 2003).

Table 2 summarises a classification of the Holocene facies of the delta proposed by Goodbred and Kuehl 2000a) based on borehole samples. Among the five Holocene facies identified by them, one—Facies-V—is exclusive to the Sylhet basin. The GBD proper, therefore, consists of four major Holocene layers deposited on an oxidised, lateritic low-stand base. From bottom to top, these are Sands, Lower Delta Mud, Muddy Sand and Thin Mud. The Sundarban sediments as well as the present over-bank flood deposits belong to the Thin Mud facies (Facies-VI). Goodbred and Kuehl (2000a) did not include the low-stand lag gravels in their scheme. These may also be classified as Pre-Holocene and put alongside the oxidised surface (Facies-I). The southern face of the GBD currently forms the frontier region of the Thin Mud facies atop the off-lapping accretionary wedge, to which the Sundarban belongs.

3. EVOLUTION OF THE SUNDARBAN REGION

3.1 Accretion of the Sundarban

Delta-building bio-tidal processes, at the southern frontier of the GBD, was responsible for phased accretion of all sea-front islands of the Sundarban c. 5~2 ka BP (Fig. 7), from what probably was a number of disconnected incipient subtidal and intertidal shoals to the supratidal landmass it is now identified with.

Riverine sediments undergo rapid transformation as they enter the estuaries. The bulk of them are carried as colloids, or small charged particles that repel each other. This condition is broken down by the electrolytes and organic matter present in the seawater and the grains start to flocculate and settle. In the still water period at the high water level of a tidal cycle, individual or groups of flocs settle on the bed of a stream or mudflat and get slowly consolidated during the subsequent slack water period. During the next tidal cycle, velocity of the mid-tide currents may not be sufficient enough to erode all the materials deposited previously. In the continuous cycles of tidal deposition and erosion, accretion only occurs if a net edge of deposition exists over erosion (Dyer, 1979; Barnes, 1984; Furukawa, *et al.*, 2014).

As the shoals formed by tidal deposition start to emerge above the low tide line, pioneer mangrove species like *Porteresia coarctata* soon start to colonise on the muddy tidal flats and the bio-tidal accretional processes take over. According to the 'classical successional view of mangrove dynamics' (Sneadaker, 1982:111), plant communities such as these literally 'prepare the ground' for the next community as they raise the level of the shoal by inducing sedimentation and thereby reducing the tidal inundation time of a particular locality. At the

end of the process, a climax — largely non-mangrove — vegetation community evolves as the land is raised sufficiently above the tidal limits (Chapman, 1976; Thom, 1984) (Fig. 8). There are many processes how the mangroves can induce an increased level of tidal accretion. For example, their stems often cause eddies that trap sediments. The sticky algal mats that develop under the plant cover can also do the same. Apart from processes like these, the entire surface of the colonising mangrove species becomes an area for sediment deposition during their inundation. This sediment is contributed to the accreting land surface when the veneer gets dry and then flecks-off during their subsequent low tide exposition (Pethick, 1984).

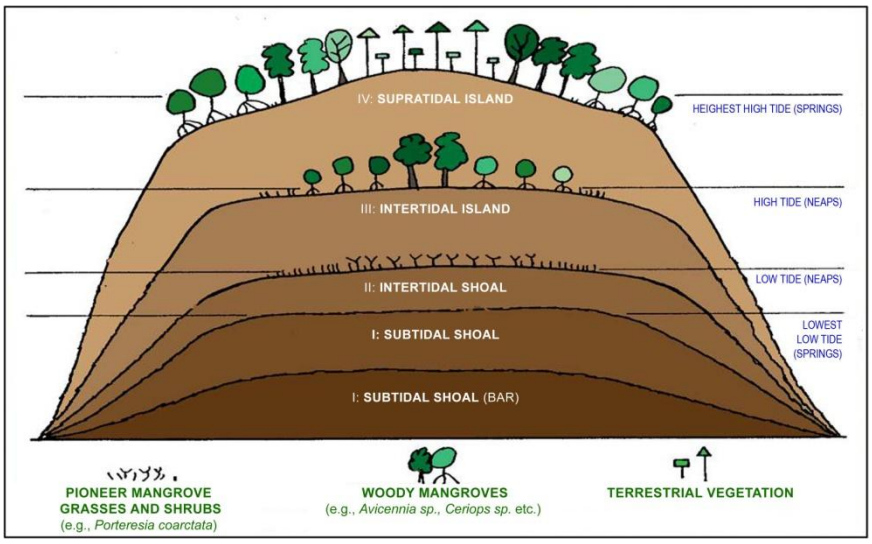

Figure 8: Stages of biotidal accretion in a tropical delta. The process starts from colonisation of grasses, herbs and shrubs that help to stabilise intertidal shoals. With rise in elevation, interval of tidal inundation reduces, and leads to successive changes in mangrove species. At maturity, the shoal evolves into a supratidal island with non-mangrove climax vegetation that is inundated only during episodic storm surges. *Source*: after Untawale and Jagtap (1991)

One problem with the succession model of mangrove ecology is that it is only observable in prograding shores, where a regressive stratigraphic order is accreted (Tomlinson, 1984:19). The scheme is difficult to apply in areas where the coastline is primarily eroding for a long time, as in the southern Sundarban. However, newly emerged tidal islands of the region do show vegetation succession. For example, the Nayachar island (47.6-km^2: 21°55'–22°01'N, 88°03'–88°09'E), situated in the upper reaches of the Hugli estuary, progressively accreted during 1948–2008 and developed four semi-concentric vegetation zones that distinctly coincide with growth stages of the island and relate to environment gradients like decreasing inundation-interval and fining-upward sediment characteristics (Bandyopadhyay, 2008).

3.2 Reclamation and present status of the Sundarban

Although the frontiers of the Sundarban mangroves started to move southward for expansion of rice farms from the 13th century (Eaton, 1990), forests still occupied ~15,000 km^2 of tidal seaface of the GBD between the Hugli and the Meghna estuaries about 240 years ago (Rennell, 1779). Rennell reflected in 1781 that ‘this tract ... is so completely enveloped in woods, and infested with tygers [sic], that if any attempts have ever been made to clear it (as is reported) they have hitherto miscarried’. He noted that ‘sand and mud banks ... extend twenty miles off some of the islands’ of the delta and contemplated that ‘some future generation will probably see these banks rise above water, and succeeding ones possess and cultivate them!’ (Rennell, 1788:259, 266).

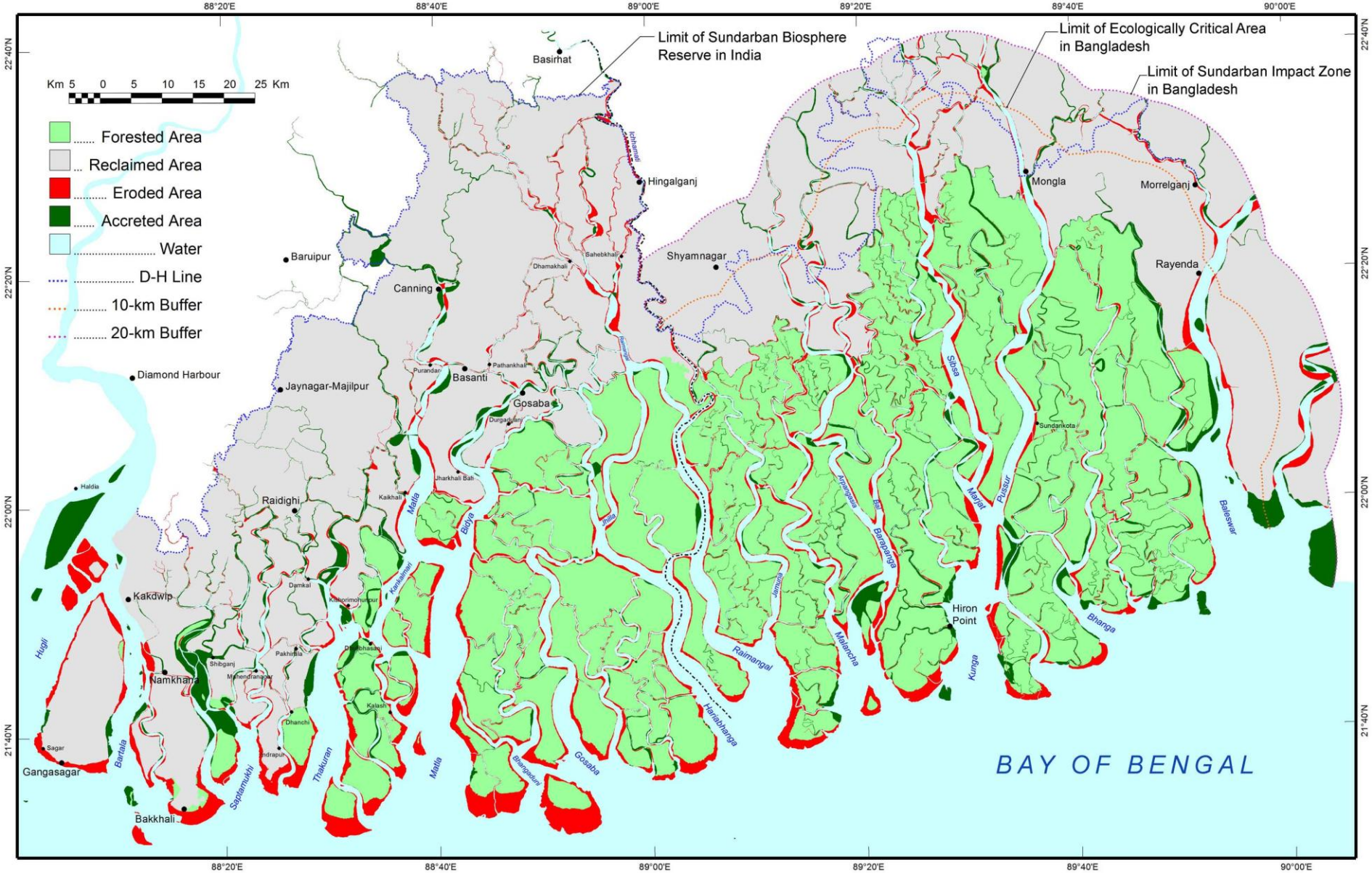

Figure 9: Composite map of the Sundarban. 1829-30 extent of the mangrove wetlands is indicated by the Dampier–Hodges (D–H) Line that is still regarded as the northern limit of the Sundarban region in India. In Bangladesh, Sundarban refers to the forests only, with its impact area demarcated by two buffers. Comparison between 1901–23 topographical maps and 2013–15 satellite images brings out the extent of erosion along nearly the entire seaface of the delta and accretion in the interior parts, mainly in the west. Tide stations referred to in Fig. 10 are also shown in the map, as are selected populated places. *Source*: coastline and channel banks extracted from 37 mosaiced Survey of India 1:63,360 topographical maps of 1901–23, belonging to 79B, C, F & G series; Landsat 8 OLI 15-m panfused data of 17 Mar 2015 & 8 Mar 2015 (for Bangladesh part); IRS-R2 LISS-4fx 5.6-m data of 23 Feb 2013 & 1 Jan 2014 (for India part). D–H Line extracted from 1:253,440 *Atlas of India* Map #121 & 122 of c. 1860

Table 4: Generalised classification of landforms in the islands of Sundarban

LANDFORM SYSTEM	BROAD GENETIC MORPHOTYPES	LOCATION	MATERIALS	DOMINANT PROCESSES	LANDFORM UNITS				GEOMORPHIC HAZARDS
					SCALE [1]	FEATURE(S)	PERMANENCY [2]	SYSTEM OF CHANGE	
I: COAST (area: ~5%)	**1**. Beach	Outer (seaward) strand of the southern islands	Mostly very fine sand (sub-angular to sub-rounded; well-sorted; positively skewed and mesokurtic) and, in eroding sections, beach clay sequences formed of sticky grey clay associated with old mangrove trunks, roots and pneumatophores	Marine erosion and deposition; Bioturbation	S	(i) Bedforms like ripples, rills and swash-marks; Mud balls; Bioturbation structures	D–E	(i) Individual forms change with every tidal cycle but the overall pattern may emerge unaltered or change slowly over the years with changing sedimentological character / flow conditions.	Coastal erosion; breaching of embankments and other coastal structures in reclaimed sections
					M	(ii) Beachforms like megaripples. Cusps and horns over sands	C	(ii) Changes slowly with changing sedimentological environment and wave conditions over the year.	
					L	(iii) Beachforms like ridges, runnels, berms and tidal sandflats. Clay windows, occasionally with sea-facing cliffs	C	(iii) From and dissipate or change in size and extension with annual cycles of wave environment and tidal conditions	
	2. Dune (Aeolian)	Back of the beaches. Not present in eroding sectors	Mostly very fine sand (sub-rounded to sub-angular; positively skewed and mesokurtic)	Aeolian erosion and deposition; biostabilisation; storm / tidal overwash. Anthropogenic modification in reclaimed stretches	S	(i) Bedforms like aeolian ripples	E	(i) Extremely responsive to aeolian transportation, can be destroyed by slightest interference	Dune progradation and deposition of wind-blown sand onto interior areas of reclaimed stretches
					M	(ii) Sandforms like barchanoid embryo dunes or neo-dunes	C	(ii) From in the late pre-monsoon and dissipate in the monsoon with annual cycle of wind regime	
					L	(iii) Sandforms like dune humps, transverse fore and back dunes, blow-outs, dune slacks. Aeolian sandflats	B–C	(iii) Initiated regionally by vegetation or coastal embankments. Parts of foredunes are wave-eroded during spring tides and / or storms while parts of back dunes transgress landwards during the pre-monsoon. Other forms are bio-stabilised and change slowly	
	3. Beach–bank transitional (tidal / fluvio-tidal)	At the mouths of seafacing estuaries and tidal inlets	Very fine sand – properties same as 1 above.	North-directed longshore drift, bioturbation in intertidal areas	S	(i) Bed forms like ripples, rills and bioturbation structures	D–E	(i) Same as 1(i) and 2(i) above	Storm erosion
					M-L	(ii) Megaripples, sandflats, mudflats	C–D	(ii) Same as 1(ii) and 2(ii) above	
	4. Estuary bank (tidal / fluvio-tidal)	Along the sides of the estuaries and tidal channels	Sticky grey clay to silty clay, hard when dry, traces of old mangrove vegetation may be present	Mostly tidal. Fluvial influence present in channels connected with up-country rivers	S	(i) Biogenic forms, rills over mudflats	D	(i) Same as 1(i) above	Same as 1 above
					M-L	(ii) Clay forms like slip-face and mudflats	B–C	(ii) Changes episodically mainly during the monsoon and / or cyclonic storms	
II. ISLAND INTERIOR (area: ~95%)	**5**. Interdistributary estuarine swamp (bio-tidal)	Inner parts of all tidal island where mangroves are present	As above – characterised by thriving mangroves / mangrove marshes. Greyish-black less-sticky clay over mudflats	Tidal and biotic accretion in different cycles (diurnal to equinoctial) of tidal inundation and storm surges	S	(i) Biogenic forms, features associated with mudflats	D	Same as 1(i). above	Storm inundation / erosion
					M–L	(ii) Creek bed and banks, inter-creek mangrove swamps / marshes, mudflats, saline blanks	B	Accretes vertically with bio-tidal accretion	
	6. Inter-creek reclamation (bio-tidal / anthropogenic)	Almost whole of the supratidal interior areas	As above – traces of old mangrove roots and pneumatophores abundant. Soil types are mostly Entisol (Fluvaquent) and Inceptisol (Haplaquept).	Anthropogenic modification (agriculture, aquaculture). Storm surge inundation.	L	Embanked deltaic plain with palaeochannels. Surface elevation lower than High Water Level Springs	A	Natural bio-tidal processes non-operative due to embanking. Changes extremely slowly with tectonic / eustatic modification and eutrophication of abandoned channels. Rare storm inundation due to overtopping or breach in marginal dykes induces some vertical accretion	Storm surge inundation, coastal erosion. Sand encroachment in southern sections of seafacing reclaimed islands

NOTES: **1**. S: small, M: medium, L: large. **2**. Permanency is indicated by 5-point scale A–E (A: most permanent, E: most ephemeral)

Under the colonial government, reclamation of the Sundarban was initiated in 1770. It transformed into an institutionalised effort from 1783 (Pargiter, 1934) manifesting administrative policies that viewed the wetlands mostly as wastelands (Richard and Flint, 1990). By 1831, reclaimable portion of the region between the Hugli and the Pussur was divided into 236 compartments or 'lots' south of the Dampier–Hodges (D–H) Line, surveyed in 1829-30 to demarcate the contemporary frontier of the wetlands (Pargiter, 1934). The scheme was later extended up to the Baleswar by adding 22 more lots. This formed the basis of all subsequent reclamation efforts (Ascoli, 1921)

Among the three original Sundarban districts, deforestation of the eastern Bakarganj was almost complete by 1910 (Jack, 1918). Situated between the Baleswar and the Meghna, the deltaic distributaries of this part have lower tidal range than the west and receive freshwater from upcountry sources. This helped to reduced salinity and replenishment of fertile sediments that sustained agriculture. In contrast, reclamation continued up to the 1980s in the western 24 Parganas, even if sporadically. Occupying the abandoned part of the GBD between the Hugli and the Raimangal, here the salinity as well as the tidal range is higher than the east, requiring higher embankments to arrest tidal spill. Between these two regions, the forests of the Khulna, bounded by the Raimangal and the Baleswar, were never subjected to the scale of reclamation seen in Bakarganj and 24-Parganas. Realisation of the commercial importance of mangroves enforced Government protection in varying degrees since 1875 in Khulna and the adjacent part of 24-Parganas (Ascoli, 1921, Curtis, 1933). As the contemporary Survey of India maps indicate, extent of mangroves in Khulna did not reduce appreciably after 1920s.

At present, the coastal region between the Hugli and the Baleswar is referred to as the Sundarban. In India, the Sundarban Biosphere Reserve is defined administratively by the 19 development blocks south of the D–H Line and includes both reclaimed and non-reclaimed parts. In Bangladesh, Sundarban represents only the forests. A 10-km and a 20-km buffer from the forest boundary designate the Ecologically Critical Area and the Sundarban Impact Zone (SIZ), respectively (Fig. 9).

Embanking the coastline and major channel banks, apart from completely blocking the smaller creeks to prevent inundation of the interior areas from highest high tide or storm surges, had been the usual reclamation procedure of the Sundarban. The indigenously designed earthen dykes required extensive annual maintenance and offered little protection against storms (Hunter, 1875). While they essentially remain unchanged in many areas in the western (Indian) Sundarban, in the east (Bangladesh), extensive areas in the SIZ are protected by large-scale polder construction since the 1960s (Bari Talukdar, 1993).

3.3 Landforms

Morphology of a deltaic coast represents the interactions between sediments brought in by the rivers, and their reworking by the tidal and wave processes that increase manifold during storms. Generated by the winds, the waves give rise to different types of currents that work on a coast longitudinally, transversely or obliquely. Tidal rise and fall change the site of wave action besides generating huge volume of water, called tidal prisms that enter and leave the coastal plains twice a day. Relative dominance of these processes determines the assemblage of landforms seen in a coast (Reading and Collinson, 1996). With amplitudes raging from 3~4 m at the estuary mouths and 4~7 m in the interior, tides play a crucial role in landform development in Sundarban. Landforms produced by winds and waves are less important and are restricted to its southern fringe (Table 4).

3.4 Coastal forcings

3.4.1 Tides

In Sundarban, the tidal cycle is semi-diurnal with minor diurnal inequality. As the high water moves in along the estuaries, it is complicated by the resonance and other factors that break down any straightforward pattern in the magnitude of tidal rise and fall. Along the seaface of the GBD, the lowest tidal range is recorded at the mouth of the Pussur estuary (Hiron Point, 2.95 m). The range increases towards its flanks at the mouths of the Hugli (Sagar island, 4.32 m) and the Meghna estuaries (Sandwip, 6.01 m). Besides this, the increasing landward morphological constriction of the hypersynchronous estuarine channels also induces the tidal range to increase northward, up to 2.5 m in some sections (Fig. 9A). The Sundarban tides are also asymmetrical with pronounced flood dominance. This means that the rising tide occupies shorter time in a cycle, inducing faster landward velocity of the bidirectional tidal current that turns the estuaries into sediment sinks. Like the tidal range, the asymmetry also amplifies northward, suggesting an increasingly higher rate of sedimentation in the upper part of the estuaries (Fig. 9B). Called tidal pumping (Postma, 1967), the net inflow of sediments has profound implication on vertical accretion Sundarban region (see section 3.5.3) which receives little or no sediment discharge from the up-country rivers barring the Hugli and the Baleswar.

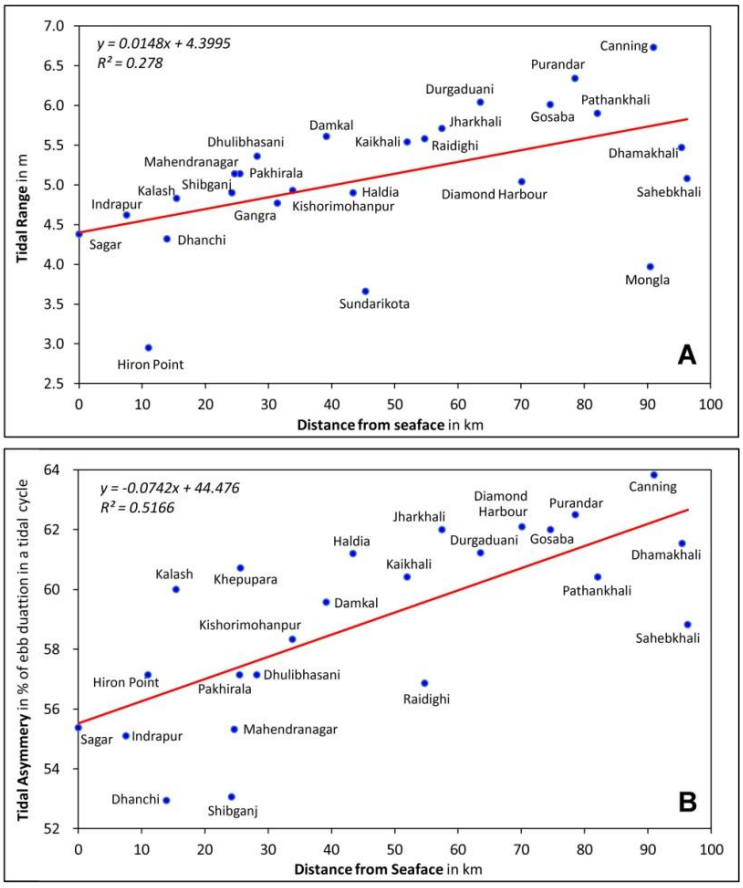

Figure 10: Tidal characteristics of the lower GBD at or close to the Sundarban region. (**A**) Landward amplification of tidal range (n=26). Sagar, Gangra, Haldia, and Diamond Harbour are situated along the Hugli estuary. Hiron Point, Sundarikota, and Mongla are situated along the Pussur, where the tidal range is comparatively lower. *Source*: SoI, 2015 (Hugli estuary stations); Chatterjee *et al.*, 2013 (Indian Sundarban stations); BIWTA, 2015 (Bangladesh stations). (**B**) Landward enhancement of tidal asymmetry (n=24). All stations shown in (A) are not represented due to non-availability of data. See Fig. 9 for location of stations. *Source*: SoI, 2015 (Hugli estuary stations); Chatterjee *et al*., 2013 (Indian Sundarban stations); UoH-SLC, 2015 and BIWTA, 2016 (Bangladesh stations)

3.4.2 Climate

The rhythm of the seasons, reflected in the yearly cycles of wind, temperature, and precipitation regimes, has an important bearing on the tidal and supratidal landforms of the Sundarban. In general, wind speeds decrease eastward. Highest south and southwesterly wind velocities are observed in the exposed western part of the region (~25 km h^{-1}) during April and May, which, coincided with the hottest (30 °C, also dry) period of the year, bring about significant changes in the morphology of sandforms in the southern seafacing islands. The southerly gusts continue through the rainy monsoon season (June–September). This is the time when, becoming moist with consistent precipitation, sand-movement stops but a freshet-induced rise in the local mean water level joins hand with wind-beaten waves and tropical cyclones to increase the intensity of coastal erosion and reworking of tidal sediments. From October, the winds start to alter their direction and speed (northerly, ~5 km h^{-1}), the wave climate also undergoes significant change and, with the onset of the winter, depositional processes take over the beaches (IMD, 1983; FAO-UN, 1985). Basing on these observations, a year in the region can be classified into the pre-monsoon (February–May), monsoon (June–September) and post-monsoon seasons (October–January). These temporal units, with their clearly defined climate and tidal conditions form the basis of observing the medium and large scale landforms of Sundarban that often follow an annual rhythm.

3.4.3 Cyclones

A six-hour pounding by the waves during a full-blown tropical cyclone can be equivalent to many years' worth of normal wave action. The destructive action of a cyclone is mostly felt on the right of its track (northern hemisphere) and on the islands that face an advancing system perpendicularly (Coch, 1994). Working on the gently sloping shelves of the GBD, the winds associated with a cyclone whip-up waves that pile water against the coast and culminate in storm surges capable of completely inundating small low-lying islands of the Sundarban. Cyclones, being low pressure systems, are reciprocated by a rise in the sea surface elevation: approximately one cm for every mb of pressure fall (Walker, 1983). As a storm surge moves into the interior, its levels are further augmented by the northward squeezing estuaries of the region. In the reclaimed Sundarban, properly maintained marginal dykes provide reasonable protection against the highest level of spring tides. However, chances of their overtopping greatly increase if the landfall of a storm coincides with the regional high water level. For example, the tropical storm Aila made its landfall in the western Sundarban on 25 May 2009 between 1:30 and 2:30 pm India Standard Time. This matched closely with spring high water and caused widespread inundation of the region although the storm was a relatively low-power system with its highest sustained wind speed of 112 km hr^{-1} (IMD, 2010).

For the north Indian ocean region, Fifth Assessment Report (AR5) of the Intergovernmental Panel for Climatic Change estimated that the frequency of tropical cyclones are likely to remain unchanged with rains getting more extreme near the centres of the storms (IPCC, 2013:1250). Specifically for the Sundarban, landfalling trend of cyclones indicates a decreasing tendency for the last few years. If the landfall events of the last 125 years are categorised into five 25-year intervals, the 1991–2015 period, with least number of recorded events, closely matches 1891–1915 at the start of the record. The 1941–1965 and 1966–1990 periods registered maximum number of landfalls of all storms, and maximum number landfalls of severe storms, respectively (IMD, 2012; http://www.rmcchennaieatlas.tn.nic.in) (Fig. 11). Operation of natural cycles in landfall frequency and harming potential of tropical cyclones is not uncommon (Coch, 1994). This, coupled with global warming-induced intensification of the storms (Webster, 2005), suggests that the probability of cyclone

landfalls and consequent damages are likely to increase in the Sundarban even if their global frequency remains unchanged.

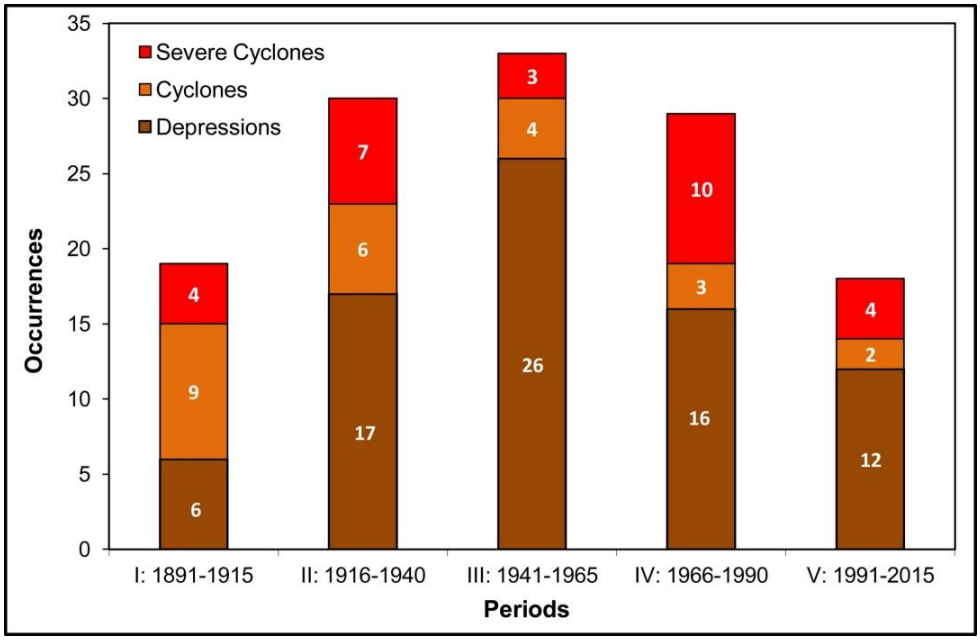

Figure 11: Tropical cyclones landfalling in the Sundarban region between 88° and 90° E. Trends indicate that a future rise in frequency in probably imminent. *Depression*: a storm with 10-min average wind speed of 31–61 km h^{-1}; *Cyclonic Storm*: 62–88 km h^{-1}; *Severe Cyclonic Storm*: >89 km h^{-1}. *Source*: <http://www.rmcchennaieatlas.tn.nic.in>

3.4.4 Sea level rise

The estuaries are particularly sensitive to changes in the MSL because, apart from enhancing vulnerabilities to erosion and storm inundation, it alters tidal forcing and influences sedimentation by setting up flood-dominated tidal asymmetry (Dyer, 1995; Goodbred and Saito, 2012). According to the IPCC AR5, the relatively low mean rates of SL rise since ~2 ka BP picked up again during the 19th century (1901–2010) at 1.7 mm a^{-1} and escalated to 3.2 mm a^{-1} between 1993 and 2010. The AR5 held the human-induced global warming responsible for this accelerated increase, and suggested a rise rate of 8–16 mm a^{-1} by the turn of this century according to one of its future scenarios (IPCC, 2013:1139).

Global geocentric MSL data obtained from satellite altimetry during Dec 1992 – May 2016, and processed by different groups, indicate an average trend from +2.9 ± 0.4 mm a^{-1} (www.star.nesdis.noaa.gov/sod/lsa) to +3.4 ± 0.4 mm a^{-1} (sealevel.colorado.edu, www.aviso.altimetry.fr). From the seasonal-signal-removed data available at sealevel.colorado.edu, SL rise in the Bay of Bengal can be estimated at +3.30 ± 0.13 mm a^{-1}. These are somewhat lower than the value obtained from the raw data for the sea adjacent to the Sundarban: +3.90 ± 0.46 mm a^{-1} (Tile 22°N/88°E, Data up to May 2016).

Trends of relative mean sea level (RMSL) changes are obtained from tide gauge records and reflect vertical land movements, if any, at the gauging points. While their data often prove anomalous to secular trends due to a number of factors (Mörner, 2010a), the RMSL values may provide an indication of land level changes at a deltaic locality and can be compared with rates of vertical accretion through sedimentation. Despite some authors maintain that a 20-year record of average annual data is adequate for estimating rates of SL change (Warrick and Oerlemans, 1990), a 50-year repository is considered more consistent for offsetting all local and short-term deviations like influences of El Niño / Southern Oscillation and tropical

cyclones (Pirazzoli, 1996; Pugh, 2004). Among the six usable Permanent Service for Mean Sea Level (PSMSL: www.psmsl.org) stations of the coastal GBD around the Sundarban, only the Sagar and Diamond Harbour record spans of 48 a and 64 a, respectively (Table 5). The rest span between 21 a (Hiron Point) and 41 a (Haldia) with even lower number of data points. Data from three other stations obtained from Sarwar (2013) and Pethick and Orford (2013) are also shown in Table 5.

Table 5: Trends of relative mean sea level from tidal observatories of the coastal GBD in the vicinity of the Sundarban

Station (with channel location)	**Period covered** [1,6,7]	**Available annual data** [1, 6, 7]	**Distance from sea** (km) [2]	**Estuary or channel width** (km) [2]	**Tidal range** (m) [3, 4]	**MSL change due to glacio-isostatic** (GI) **rise** (mm a^{-1}) [5]	**RMSL trends without adjusting for GI rise** (mm a^{-1}) [1, 6, 7]
Diamond Harbour (Hugli)	1948–2011 (64 a) [1]	62 a [1]	70.1	1.88	5.04 [3]	–0.35	+3.97 ± 0.34 [1]
Haldia (Hugli)	1971–2011 (41 a) [1]	38 a [1]	43.4	10.47	4.90 [3]	–0.34	+2.67 ± 0.49 [1]
Gangra (Hugli)	1974–2006 (33 a) [1]	27 a [1]	31.4	17.25	4.77 [3]	–0.33	+1.19 ± 0.76 [1]
Sagar (Hugli)	1937–1988 (48 a) [1]	48 a [1]	2.3	51.58	4.38 [3]	–0.30	–2.98 ± 0.93 [1]
Khepupara (Nilganj)	1979–2000 22 a) [1]	18 a [1]	25.6	0.31	3.73 [4]	–0.28	+19.15 ± 2.18 [1]
Hiron Point (Pussur)	1983–2003 21 a) [1]	21 a [1]	11.0	6.91	2.95 [4]	–0.28	+3.56 ± 2.13 [1]
Mongla (Pussur) [6]	1998–2010 (13 a) [6]	13 a [6]	90.5	1.02	3.97 [4]	—	+6.25 [6]
Amtali (Payra) [7]	1958–2002 (45 a) [7]	45 a [7]	44.2	1.81	—	—	+3.16 [7]
Rayenda (Baleswar) [7]	1969–2001 (33 a) [7]	31 a [7]	51.3	2.42	—	—	+3.64 [7]

Notes: **A**. The PSMSL data occasionally undergo correction, updating, and addition that affect the trends derived from them. **B**. The basic dataset is available in Revised Local Reference (RLR) datum, which is approximately 7 m below the mean sea level. **C**. RMSL data of Sagar and Khepupara are anomalous from the regional trends and may not represent actual conditions (see text for explanation).

Source: **1**. www.psmsl.org, retrieved on 2016-05-30; **2**. L8 OLI images of 2015; **3**. SoI (2015); **4**. BIWTA (2015); **5**. Glacio-isostatic rise values from Richard Peltier's VM-2 model: <http://www.psmsl.org/train_and_info/geo_signals/gia/peltier/drsl250.PSMSL.ICE5Gv1.3_VM2_L90_2012b.txt>; **6**. Data of Mongla from Orford and Pethick (2013), originally sourced from Mongla Port Authority; **7**. Data of Rayenda and Amtali from Sarwar (2013), originally sourced from Bangladesh Water Development Board

The records at Sagar show a falling RMSL, which do not agree with the continuous coastal erosion documented around the tidal observatory for decades (Bandyopadhyay, 1997), denoting some problem with the gauge data. Khepupara (+19.15 mm a^{-1}), on the other hand, records an anomalously high rate of RMSL rise, which suggests subsidence at this locality. Notwithstanding issues with constancy of the tide gauges (Mörner, 2010b), the RMSL trends at Amtali (+3.16 mm a^{-1}), Hiron Point (+3.56 mm a^{-1}), and Rayenda (3.64 mm a^{-1}) are not overtly different from the regional secular SL trends obtained from satellite altimetry (+3.3~3.9 mm a^{-1}). This indicates some stability at these sites and is not inconsistent with the millennium scale RMSL change of +1–4 mm a^{-1}, estimated for the eastern Sundarban through core analysis (Allison and Kepple, 2001).

RMSL trends from Gangra (+1.19 mm a^{-1}) through Haldia (+2.67 mm a^{-1}) and Diamond Harbour (+3.97 mm a^{-1}) show a progressive landward increase along the Hugli estuary (Fig. 12). This may be accounted for by the fact that the increasingly smaller cross-sectional area of the north in the flood-dominated Hugli (Column 5 of Table 5) is filling-up at a faster rate than

its southern sections, causing mean tidal levels to rise at a progressively higher rate in the landward direction (Nandy and Bandyopadhyay, 2010). Similar observation is also made along the Pussur, between the seaface-located Hiron Point (+3.56 mm a^{-1}) and the interior Mongla (+6.25 mm a^{-1}). The Mongla data, however, spans only for 13 years and may not be very reliable.

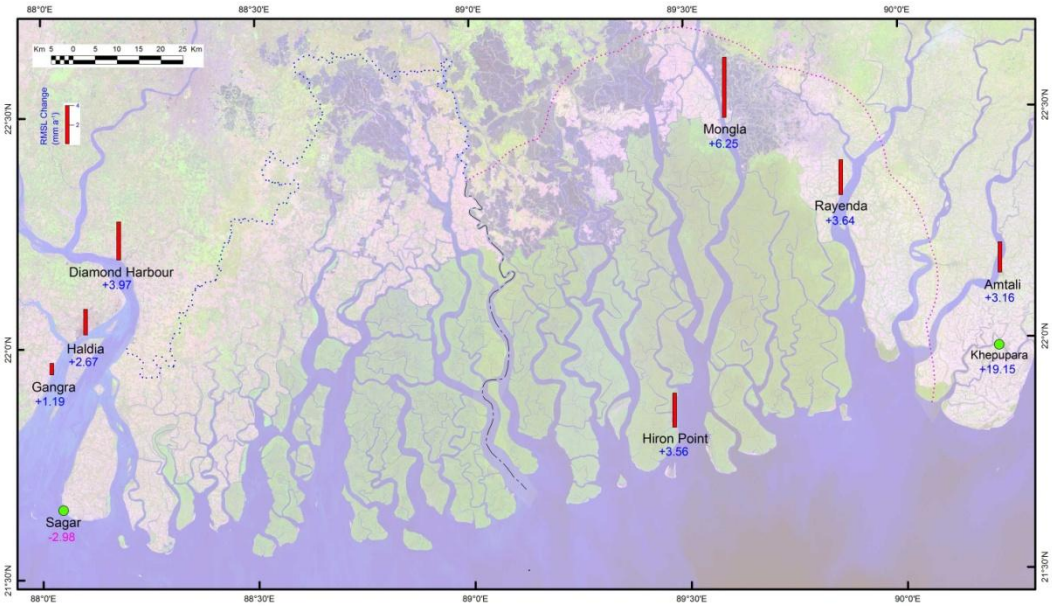

Figure 12: Available RMSL trends (in mm a^{-1}) in the coastal Ganga–Brahmaputra delta at or close to the Sundarban region. Data of Khepupara and Sagar are not represented by bars because of their anomalous values. Blue and magenta dotted lines denote the limits of the Sundarban Biosphere Reserve in India and Sundarban Impact Zone in Bangladesh, respectively; black line is the international boundary. *Source*: see Table 5

3.5 Coastal changes

3.5.1 Mapping history

James Rennell's 18th century map of the Bengal was compiled from some 500 different surveys conducted by himself, his associates and others. By 1777, these were first combined in a map of 1:316,800 (5 miles to an inch), and was later used to produce a set of 16 sheets that, in turn, were utilised in putting together his 1:633,600 (10 miles to an inch) *Bengal Atlas*, the first edition of which was published in 1779 and the second in 1781 (Hirst, 1917). The Sundarban and the coastal areas of the western GBD in Rennell's map were actually surveyed by his associate John Ritchie during 1769–73. Because of planimetric inaccuracies, it is impossible to georeference Rennell's maps reliably and their value lies mainly in qualitative assessment of past position and configuration of the mapped features (Hirst, 1917:26, 43). The next depiction of the delta front was R. Lloyd's 1842 *Sea Face of the Soondurbans* (1:253,440, 4 miles to an inch), based apparently on astronomical observations. This was followed by the 1:253,440 Map # 121 and 122 of the *Atlas of India* series, surveyed and produced by the Survey of India (SoI) in c. 1860. The standard 1:63,360 (one inch to a mile) 15′×15′ topographical maps representing Sundarban were started to be surveyed from 1901. The entire region was covered in 37 individual sheets by 1923. Some of these maps ran up to two to three revised editions during the following two decades. For the Indian part of the Sundarban, the 1:63,360 topomaps were replaced by the 1:50,000 (2 cm to a km) series, surveyed during 1967–1969. From this time onward, regular availability of satellite images including the 1967 Corona space-photos ushered in the possibility of continuous monitoring and mapping of changes in a digital environment.

3.5.2 Characteristics of change

Sherwill (1858) was probably the first worker to deal with the progradation of the GBD. Estimating the sediment discharge rate of the Ganga–Brahmaputra as 1,133 × 10^6 m^3 a^{-1}, he speculated that at this rate the delta should have advanced many kilometres into the sea. He also identified the Swatch of No Ground submarine canyon that cuts across the GBD shelf to reach 30 km off the Kunga estuary, as the principal silt-trapper, retarding delta growth. Contemporaneously, Fergusson (1863:351.) concluded that, though the eastern half of the GBD is 'in a state of rapid change', 'little or no change or extension seaward has taken place, during the last 100 years' in the Sundarban sector. Later, Reaks (1919) superposed and compared the maps of Lloyed (1842) and SoI (~1910) for the entire delta face and had clearly brought out the eroding nature of the Sundarban section. This trend, detected a century ago, is reflected in many recent studies and estimates of coastal change related to the Sundarban (e.g., Chakrabarti, 1995; Bandyopadhyay and Bandyopadhyay, 1996; Allison, 1998; Hazra *et al.*, 2002; Bandyopadhyay *et al.*, 2004; Ganguly *et al.*, 2006; Rahman *et al.*, 2011; Rahman, 2012; Sarwar and Woodroffe, 2013; Raha *et al.*, 2014; Chakrabarti and Nag, 2015; Ghosh *et al.*, 2015 etc.). None of these works, however, cover the entire Sundarban region beyond a few kilometres north of the seaface and mostly have either been confined either to the west (Indian) or to the east (Bangladeshi) of the Raimangal–Hariabhanga.

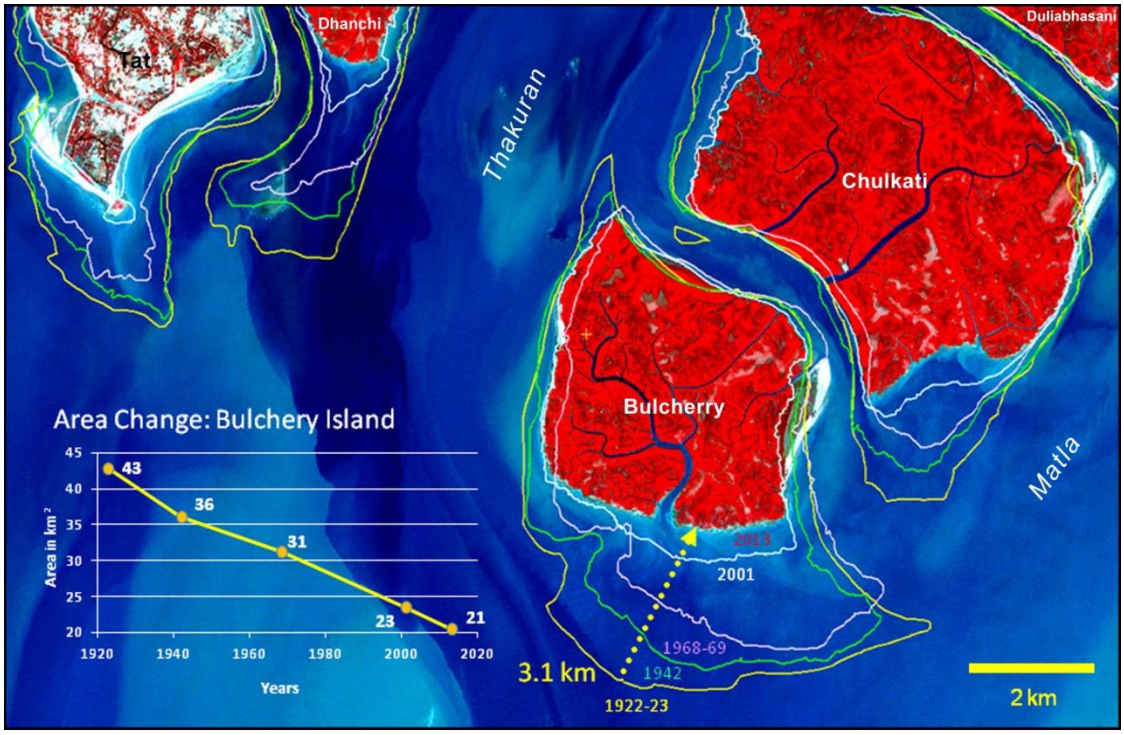

Figure 13: Coastal retreat in the Sundarban is highest between the Saptamukhi and the Hariabhanga estuaries. Here the Bulchery is represented to show relentlessness of the erosion through different years. Like other sea-facing islands of the area, its area reduced by 50% within the last 100 a and is likely to get obliterated within the next 100 a or so. *Source*: 1922-23 & 1942: SoI 'inch' topomaps #76C/06 on 1:63,336 (two editions); 1968-69: SoI 'metric' topomap #76C/06 on 1:50,000; 2001: IRS-1D LISS-3+Pan 5.6-m data of January 2001; 2013 (base image): IRS-R2 LISS-4fx 5.6-m data of 23 Feb 2013

If the drainage and high water lines of SoI's 1901–23 'inch' maps of the Sundarban are overlaid on recent satellite images (Fig. 9), five things become apparent: • In continuation of the trend brought out by Reaks (1919), nearly the entire southern face of the region is retreating, irrespective of forested or reclaimed portions. Rate of erosion is maximum at the west-central section between the Saptamukhi and the Gosaba estuaries (Fig. 13), reaching up

to 40 m a^{-1}, and gradually reduce west- and eastward, almost to reach zero on the west bank of the Baleswar . • A number of interior creeks and estuaries are getting silted, mostly (partly) in the reclaimed western (northern) section. • Outside this region, banks of most major estuaries are eroding; the situation is somewhat mixed for the smaller creeks of the forested islands. • Fairly large sections of the western Sundarban became reclaimed in 24 Parganas. On the island level, the progressive and irreversible transformation of intra-island creeks into stagnant water bodies; their degeneration and integration into the farmlands are some of the notable post-reclamation changes that took place within an approximate span of 50 a (Fig. 14). • Conversely, a large section of the erstwhile farmlands are converted into shrimp farms, mostly in the reclaimed eastern section of the region. This gained momentum from about the 1980s.

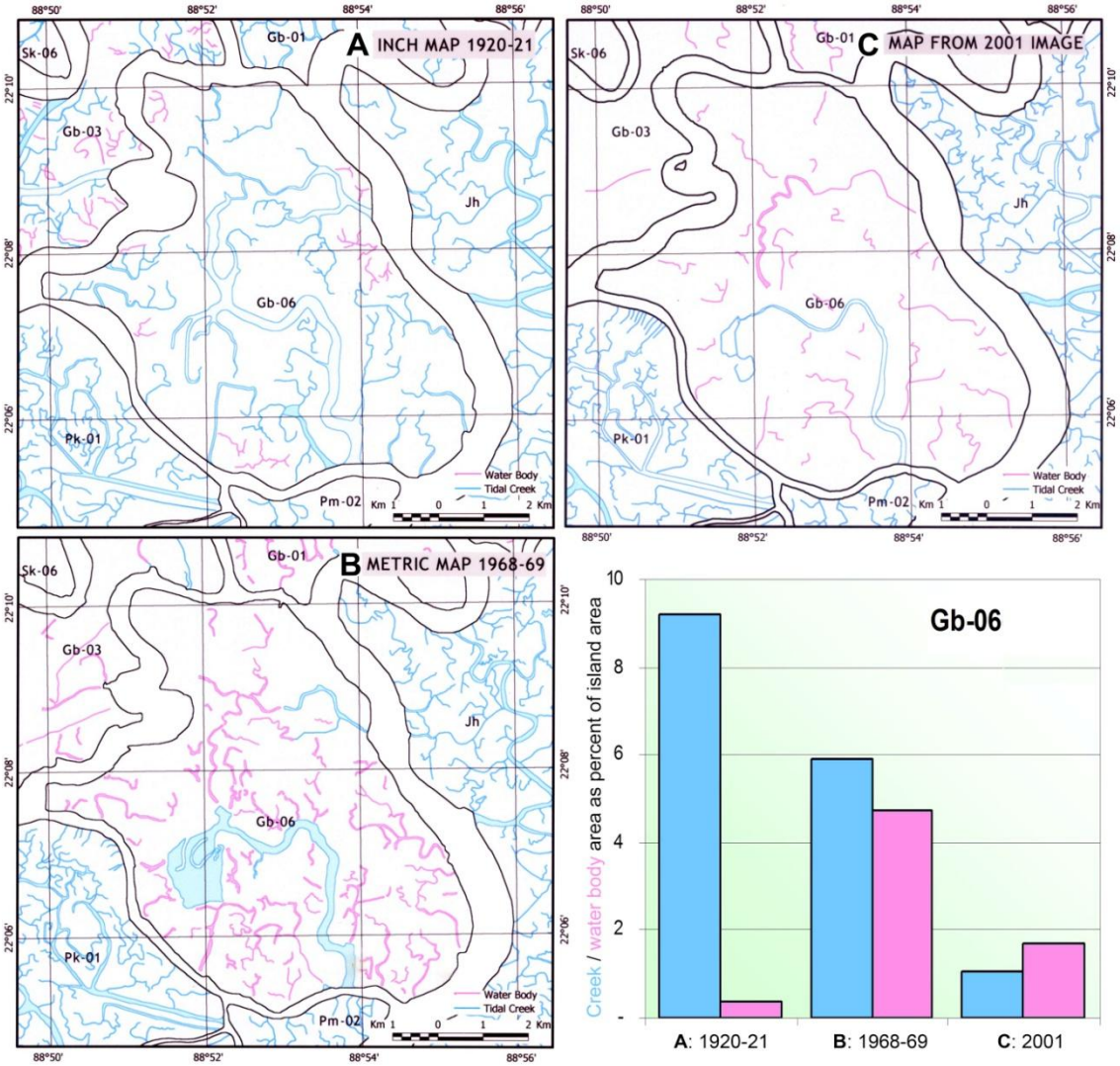

Figure 14: Transformation of tidal creeks into water bodies in Satjaliya island (coded Gb-06) of Gosaba block of western Sundarban from 1920-21 (A) through 1968-69 (C) and 2001 (D). The changes are compared in the bottom left diagram. In 1920-21, when the island was under forests, there were hardly any water bodies in the island. During its subsequent reclamation, a number of tidal creeks were blocked at their entrances and a marginal embankment was constructed all around the island and along the major channels. This transformed the free-flowing water courses to stagnant water bodies. With time, these water bodies were subjected to eutrophication and/or land-filling for expansion of farmlands or for habitational use. In contrast, none of the creeks in the adjacent non-reclaimed areas lost their original density. *Source*: (A) SoI 'inch' Map # 79B/16 on 1:63,360; (B) SoI 'metric' Map # 79B/16 on 1:50,000; (C) IRS-1D LISS-L3+Pan data of January 2001

3.5.3 Causes of change

Stability of deltaic coastlines is often a function of the accretional fluvial inputs and the erosional wave and tidal forcings. As the Sundarban forms a part of the fluvially abandoned western GBD (Fig. 1), its sediment supply must come from the tidal sources to render it any long term stability against the RMSL rise. The average annual sediment input of the Meghna estuary in the shelf region of the GBD is estimated at 10^9 t (Milliman and Syvitski, 1992), 95% of which is pulsed during the monsoons (Goodbred, 2003). As this sediment moves west during the high energy conditions between May and September, a part of it gets intercepted by the Swatch of No Ground submarine canyon and escapes southward into the deep sea Bengal fan (Kuehl *et al.*, 1989, 1997, 2005). The continuous erosion of the southern Sundarban for the last ~200 a, increasingly more towards the west (Reaks, 1919; Fig. 9, 13), points to the absence of sediment replenishment at the exterior delta and along the channel banks that take the maximum brunt of monsoon waves and tropical storms.

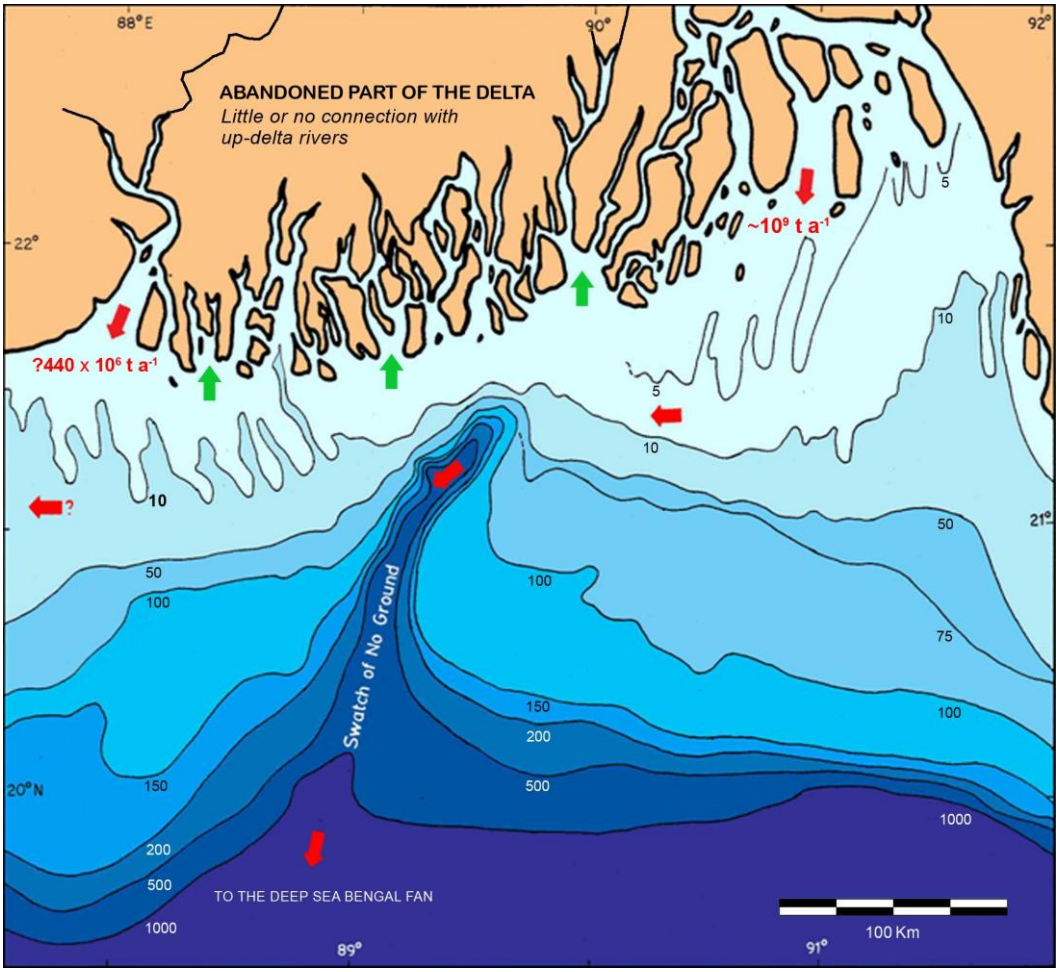

Figure. 15: Position of the Swatch of No Ground canyon in the continental shelf of the GBD. The swatch bisects the shelf region into two and acts as a conduit for interception and transportation of the Meghna sediments into the deep sea Bengal fan (red arrows). This may have augmented the lateral erosion of the coastline in the fluvially abandoned Sundarban region. It seems that most of the sediments brought by the Hugli also do not find their way into the delta. However, interior parts of the Sundarban are getting vertically accreted by tidal reworking of sediments (green arrows). *Source*: isobaths from National Hydrographic Office chart No. 31

In the west, the sediment input of the Hugli is variously estimated as 0.616×10^9 t a^{-1} (Sengupta *et al.*, 1989) and $0.473–0.481 \times 10^9$ t a^{-1} (Bandyopadhyay and Bandyopadhyay, 1996). Wasson (2003) estimated this to be upwards of 0.328×10^9 t a^{-1} without the

contribution from the Hugli's western tributaries. This means that the sediment contribution of the Hugli, although considerably smaller than the Meghna, is not insignificant. However, in contrast to the prograding eastern delta (Sarwar and Woodroffe, 2013), the century-scale retreat of the western delta coastline indicates that the Hugli sediments do not replenish its erosion and probably escape westward following the regional trend. In addition to this, the tidal range of the western Sundarban (Sagar: 4.38 m), which is 1.4 m higher than its eastern sectors (Hiron Point: 2.95 m) also aid the process. The existence of prominent tidal channels off the western Sundarban is indicated by the 10-m isobaths in Fig. 15.

Conversely, in the interior part of the delta away from the tidal channels, radioisotope geochronology and direct measurements in 2008 indicated that the island tops of the Khulna mangroves are actively accreting by tidal inundation, at a mean rate of 10 ± 9 mm a^{-1} (Rogers *et al.*, 2013). Earlier, Allison and Kepple (2001) derived similar figures (0–11 mm a^{-1}) for this region on decadal and millennium time scales. The rate of deposition was seen to be negatively correlated to the distance from seaface, implying tidal sources. These values appear to be adequate for coping with the current rates of RMSL rise (Section 3.4.4), but not sufficient to prevent *lateral* erosion seen in the seaface and along the edges of many tidal channels (Fig 9). Most of the sediments that sustain the high rate of vertical accretion are sourced from the annual monsoon pulse apart from older sediments, reworked from the creeks and the shelf. It is estimated that the Sundarban acts as a significant sink for the Ganga–Brahmaputra sediments, storing 8–10% of its annual discharge (Table 6) (Rogers *et al.*, 2013). An earlier estimate had put this at 7–13% (Allison and Kepple, 2001).

Table 6: Sediment budget of the Sundarban forests (source: Rogers *et al.*, 2013)

Province	**Surface area** (km^2)	**Storage** (10^6 t a^{-1})	**Percent of total sediment discharge of the Ganga and the Brahmaputra** [1]
Bangladesh	4,800	62.4	6.2
India	3,000	13–32	1.3–3.2
Total	8,000	77.4–96.4	8–10

Note: **1**. Total Ganga–Brahmaputra sediment discharge is estimated as ~10^9 t a^{-1} by Milliman and Syvitski (1992).

Northward increasing flood-dominance of tidal currents is common in most areas of Sundarban (Fig. 10). It has been argued that the siltation of the interior estuaries, especially in the western Sundarban, might be a response to reduction in tidal spill due to reclamation (Bandyopadhyay, 1997; Nandy and Bandyopadhyay, 2010). For maintenance of morphological steady state, length of a macrotidal (tidal range: > 4 m) estuary needs to equal a quarter of the wavelength of the tide entering into it (Wright et al., 1973). The tidal wavelength, in turn, depends critically on the mean depth of the estuaries. Construction of marginal embankments increases channel depth and accentuates flood dominance of tidal current to induce sedimentation as the channel tries to restore its equilibrium (Pethick 1994).

3.5.4. Consequences of reclamation

EFFECTIVE SEA LEVEL RISE: Using monthly averages of tide-gauge data of Hiron Point (22 a), Mongla (13 a), and Khulna (32 a), Pethick and Orford (2013) showed that, owing to the tidal range that amplified landward and over the years, the mean high water level (MHWL) along the Pussur rose at a much higher rate than the RMSL. Termed Effective Sea Level Rise or ESLR, the trend of MHWL increase at these stations were found to be 10.7, 14.5, and 17.2 mm a^{-1} as against RMSL rise of 7.9, 6.3 and 2.8 mm a^{-1}, respectively. Extensive polder formation in the 1960s reduced the tidal prism of Pussur by 10^9 m^3, cutting discharge of the channel by half. This made the landward constricting channel oversized, and decreased the frictional damping of tidal waves. Dredging operations for navigability aggravated the

situation even more, inducing tide range amplification (Pethick and Orford, 2013). Breaching or overtopping of the Sundarban embankments is mostly caused by storm surges that coincide with high water. The very high rate of ESLR would have a major concern for future flooding of the region.

Export-oriented shrimp farming received major impetus from the mid-1980s in Bangladesh (Hossain *et al.*, 2013). About 500 km^2 of reclaimed region located in the former spill area of the Pussur are converted into aquaculture farms during the last few decades and receive a large amount of discharge from the river for their maintenance. Citing example from northern reaches of the Bhagna (upper Raimangal) in western Sundarban, Bhattacharyya *et al.* (2013) stated that proliferation of shrimp farms led to an increase in tidal discharge and accelerated erosion of the embankments placed along the channel. Thus, the shrimp farms may have helped in some amelioration of the ESLR at Pussur and other estuaries in estuaries in the SIZ.

REDUCTION IN TIDAL ACCRETION: Prevention of tidal inundation in a permanently reclaimed region stops the natural process of delta building and keeps the area lower than the highest high water and storm surge levels. The region remains and forever prone to hazards like saltwater ingression and flooding due to breaching or overtopping of the embankments. This problem was recognised long ago by authors like Ascoli (1921:155), Addams-Williams (1919), and Mukherjee (1969, 1976).

Large-scale polder construction in the 1960s permanently arrested tidal inundation in much of the SIZ. Recently, Auerbach *et al.* (2015) showed that this resulted in a loss of 1–1.5 m of elevation inside the polders compared to neighbouring mangroves which continued to receive sediments through tidal inundation. Removal of forest biomass, ground compaction and ESLR also contributed to the difference. This translates into an elevation loss of 20–30 mm a^{-1} during the last 50 a inside the reclaimed region, greatly increasing its vulnerability to ESLR and storm surges. Dykes of some of these polders were breached by the tropical storm Aila in 2009 and opened them to tidal spill for up to two years before complete repairs were made. In Polder #32, located on the eastern bank of Sibsa adjacent to the mangroves, an average accretion rate of 180 mm a^{-1} was achieved during this period (Auerbach *et al.*, 2015). In Sundarban Biosphere Reserve, tidal sedimentation is used ingeniously by some 42 brick kilns that operate along the banks of the Hugli and the Ichhamati (upper Raimangal). Basins adjacent to the channels are kept open to tidal spills all through the monsoons. They are drained in the post monsoon season and the sediments, deposited at 50~100 mm a^{-1}, are utilised for brick making.

4. CONCLUDING NOTES

From an environmental view point, alteration of human activities is the most ideal option to accommodate or reverse the current transformations of the Sundarban. It seems that controlled retreat from the reclaimed stretches by relocating the resident population and embankment removal are the only long term solutions to the problem of erosion of creek margins. In many areas, bank erosion is set to aggravate with RMSL rise, and especially ESLR (Bhattacharyya *et al.*, 2013; Pethick and Orford, 2013). The very high rate of sedimentation recorded from the polders exposed to tidal inundation (Auerbach *et al.*, 2015) clearly opened up the possibility of elevation recovery in the reclaimed Sundarban through controlled or phased opening to tidal spills. In the non-reclaimed stretches, the rate of the vertical accretion (Allison and Kepple, 2001; Rogers *et al.*, 2013) seems to be adequate to keep pace with the RMSL trends detected from the region so far. In contrast to this, the retreat of the southern coastline of the Sundarban seems irreversible and future policies must take this into account. Fortunately, only four out of the 25 southern islands of the Sundarban is populated; therefore it is unlikely to make a strong impact on the humans; but its

environmental cost is undeniable. Experience from the 24 Parganas Sundarban has shown that relocation of the erosion-affected population is often impossible because of the area's high population density and growth rate. In the few cases where relocations were made, the settlers had to significantly compromise their quality of life (Chakma and Bandyopadhyay, 2012).

Research during the past two decades has brought out a number of physical trends that can be utilised to formulate a holistic plan that would address the key issues of the Sundarban. It is, however, important to filter out anecdotal and erroneous predictions from the array of new information available (Brammer, 2014). Future planning for the region must accept the change that have been introduced into the system by the humans and choose a moderate course between the requirements of the nature and the needs of the people. Organisational intervention is seldom avoidable in initiating a change, but with the present socio-political mindset of the people of the Sundarban, a take on many of its problems is only possible through benefit sharing and participatory management—a concept that has brought significant success in forest management of the western Sundarban.

Acknowledgements

I thank Nabendu Sekhar Kar, Karabi Das, Pritam Santra, and Dipanwita Mukherjee for their help in preparation of the cartographic materials. Bushra Nishat has kindly made the tide tables of Bangladesh available for this work.

REFERENCES

Addams-Williams, C. 1919. History of the Rivers in the Gangetic Delta: 1750–1918. 2001 reprint. In *Rivers of Bengal: A Compilation*, 2, West Bengal District Gazetteers, Government of West Bengal, Kolkata: 205–318.

Agarwal, R.P., Mitra, D.S. 1991. Paleogeographic reconstruction of Bengal delta during Quaternary period. In Vaidyanadhan, R. (editor): *Quaternary Deltas of India, Memoir Geological Society of India*, 22: 13–24.

Alam, M. 1989. Geology and depositional history of the Cenozoic sediments of the Bengal basin. *Palaeogeography Palaeoclimatology Palaeoecology*, 69: 125–139.

Allison, M.A. 1998. Historical changes in the Ganges–Brahmaputra Delta Front. *Journal of Coastal Research*, 14(4): 1269–1275.

Allison, M.A., Kepple, E.B. 2001. Modern sediment supply to the lower delta plain of the Ganges–Brahmaputra River in Bangladesh. *Geo-Marine Letters*, 21: 55–74.

Allison, M.A., Khan, S.R., Goodbred Jr., S.L., Kuehl, S.A. 2003. Stratigraphic evolution of the late Holocene Ganges-Brahmaputra lower delta plain. *Sedimentary Geology*, 155: 317–342.

Ascoli, F.D. 1921. *A Revenue History of Sundarbans from 1870 to 1920*. 2002 reprint, West Bengal District Gazetteers, Govt. of West Bengal, Kolkata: 218p.

Auden, J. B. 1949. Geological discussion of the Satpura hypotheses and Garo-Rajmahal gap, *Proceeding National Institute of Science, India*, 15: 315–340.

Auerbach, L.W., Goodbred Jr., S.L., Mondal, D.R., Wilson, C.A., Ahmed, K.R., Roy, K., Steckler, M.S., Small, C., Gilligan, J.M., Ackerly, B.A. 2015. Flood risk of natural and embanked landscapes on the Ganges–Brahmaputra tidal delta plain. *Nature Climate Change*, 5(2): 153–157.

Bandyopadhyay, S. 1997. Coastal erosion and its management in Sagar island, South 24-Parganas, West Bengal. *Indian Journal of Earth Science*, 24(3-4): 51–69.

Bandyopadhyay, S. 2007. Evolution of the Ganga Brahmaputra delta: A review. *Geographical Review of India*, 69(3): 235–268.

Bandyopadhyay, S. 2008. Evolution of Nayachar island, Hugli estuary, West Bengal. In Basu, R. (editor)" *Changing Scenario of Deltaic Environment*. Department of Geography Monograph No. 1, University of Calcutta, Kolkata: 89–95.

Bandyopadhyay, S., Bandyopadhyay, M.K. 1996. Retrogradation of the western Ganga-Brahmaputra delta, India and Bangladesh: Possible reasons. In Tiwari, R.C. (editor): *Proceedings of 6th Conference of Indian Institute of Geomorphologists, National Geographer*, 31(1-2): 105–128.

Bandyopadhyay, S., Mukherjee, D., Bag, S., Pal, D.K., Das, R.K., Rudra, K. 2004. 20th century evolution of banks and islands of the Hugli estuary, West Bengal, India: Evidences from maps, images and GPS survey. In Singh, S., Sharma, H.S., De, S.K (editors): *Geomorphology and Environment*, ACB Publishers, Kolkata: 235–263.

Banerjee, M., Sen, P.K. 1987. Palaeobiology in understanding the change of sea level and coastline in Bengal basin during Holocene period, *Indian Journal of Earth Sciences*, 14(3-4): 307–320.

Bari Talukdar, M.A. 1993. Current status of land reclamation and polder development in coastal lowlands of Bangladesh. *Polders in Asia, Atlas of Urban Geology*, 6, United Nations Economic and Social Council for Asia and the Pacific: 1–22.

Barnes, R.K.S. 1984. *Estuarine Biology*. 2nd edition, Edward Arnold, London: 1–11.

Bhattacharyya, S., Pethick, J., Sensarma, K. 2013. Managerial response to sea level rise in the tidal estuaries of the Indian Sundarban: A geomorphological approach. In Xun, W., Whittington, D. (editors): *Water Policy, Special Edition: The Ganges Basin Water Policy*, 15: 51–74.

Biswas, S. K., Agrawal, A. 1992. Tectonic evolution of the Bengal foreland basin since the Early Pliocene and its implication on the development of the Bengal fan. *Recent Geo-Scientific Studies in the Bay of Bengal and the Andaman Sea, Geological Survey of India Special Publication*, 29: 5–19.

BIWTA: Bangladesh Inland Water Transport Authority. 2015. *Bangladesh Tide Tables 2016*, Dept of Hydrology, BIWTA, Dhaka: 162p.

Blanford, H.F. 1864. Note on a tank section at Sealdah, Calcutta. *Journal of the Asiatic Society of Bengal*, 33(2): 154–158.

Brammer, H. 2014. Bangladesh's dynamic coastal regions and sea-level rise. *Climate Risk Management*, 1: 51–62.

Chakma, N., Bandyopadhyay, S. 2012. Swimming against the tide: Survival in the transient islands of the Hugli estuary, West Bengal. In Jana, N.C. (editor): *West Bengal: Geo-spatial Issues*, University of Burdwan, Bardhaman: 1–19.

Chakrabarti, P. 1991. Morphostratigraphy of coastal Quaternaries of West Bengal and Subarnarekha delta, Orissa, *Indian Journal of Earth Science*, 18 (3/4): 219–225.

Chakrabarti, P. 1995. Evolutionary history of the coastal Quaternaries of the Bengal plain, India. *Proceedings, Indian National Science Academy*, 61A(5): 343–354.

Chakrabarti, P., Nag, S. 2015. *Rivers of West Bengal: Changing Scenario*. Geoinformatics and Remote Sensing Cell, Govt. of West Bengal, Kolkata: 265p.

Chapman, V.J. 1976. *Coastal Vegetation*, 2nd edition, Pergamon Press, Oxford: 233p

Chatterjee, M., Shankar, D., Sen, G.K., Sanyal, P., Sundar, D., Michael, G.S., Chatterjee, A., Amol, P., Mukherjee, D., Suprit, K., Mukherjee, A., Vijith, V., Chatterjee, S., Basu, A., Das, M., Chakraborti, S., Kalla, A., Misra, S.K., Mukhopadhyay, S., Mandal, G., Sarkar, K. 2013. Tidal variations in the Sundarbans estuarine system, India. *Journal of Earth System Science*, 122(4): 899–933.

Chen, Y., Courtillot, V., Cogné, J.P., Besse, J., Yang, Z., Enkin, R. 1993. The configuration of Asia prior to the collision of India. Cretaceous palaeomagnetic constraints. *Journal of Geophysical Research*, 98: 21927–21942.

Coch, N.K. 1994. Geological Effects of Hurricanes. In Morisawa, M. (editor): *Geomorphology and Natural Hazards: Proceedings of the 25th Binghamton Symposium in Geomorphology*, *Geomorphology*, 10(1-4): 37–63.

Cochran, J.R. 1990. Himalayan uplift, sea level, and the record of Bengal fan sedimentation at the ODP leg 116 sites. In Cochran, J.R., Stow, D.A.V. (editors): *Proceedings of the Ocean Drilling Program: Scientific Results*, 116: 397– 414.

Cullen, J.L. 1981. Microfossil evidence for changing salinity patterns in the Bay of Bengal over the last 20000 years. *Palaeogeography Palaeoclimatology Palaeoecology*, 35: 315–356.

Curray, J.R. 2014. The Bengal depositional system: From rift to orogeny. *Marine Geology*, 352: 59–69.

Curray, J.R., Emmel, F.J., Moore, D.G., Raitt, R.W. 1982. Structure, tectonics and geological history of the northeastern Indian ocean. In Nairn, A.E.M., Stehli, F.G. (editors): *Ocean Basins and Margins*, 6, Plenum, New York: 399–450.

Curtis, S.J. 1933. *Working Plan for the Forests of the Sundarbans Division for the Period from 1st April 1931 to 31st March 1951*. 1, Bengal Government Press, Calcutta: 175p.

Dyer, K.R. 1995. Responses of estuaries to climate change. In Eisma, D. (editor): *Climate Change: Impact on Coastal Habitation*, CRC Press, Boca Raton: 85–110.

Dyre, K.R. 1979. Estuaries and estuarine sedimentation. In Dyer, K. R. (editor): *Estuarine Hydrology and Sedimentation*, Cambridge University Press, Cambridge: 1–18.

Eaton, R.M. 1990. Human Settlement and Colonization in the Sundarbans, 1200-1750. *Agriculture and Human Values*. 7(2): 7–16.

FAO-UN: Food and Agriculture Organization of the United Nations 1985. *Report on Tidal Area Study*. Retrieved on 2016-04-30 from <http://www.fao.org/docrep/field/003/ac352e/AC352E00.htm#TOC>.

Fawcus, L.K. 1927. *Final Report on the Khulna Settlement: 1920–1926*. Bengal Secretariat Book Depot, Calcutta: 189p.

Fergusson, J., 1863. On recent changes in the delta of the Ganges. *The Quarterly Journal of the Geological Society of London*, 19: 321–354.

Fowler, C.M.R. 1990. *The Solid Earth: An Introduction to Global Geophysics*. Cambridge University Press, Cambridge: 54–56.

Furukawa, Y., Reed, A.H., Zhang, G. 2014. Effect of organic matter on estuarine flocculation: a laboratory study using montmorillonite, humic acid, xanthan gum, guar gum and natural estuarine flocs. *Geochemical Transactions*, 15: 1–7. Retrieved on 2016-06-09 from <http://www.ncbi.nlm.nih.gov/pmc/articles/PMC3882290/>.

Ganguly, D.; Mukhopadhyay, A., Pandey, R.K., Mitra, D. 2006. Geomorphological Study of Sundarban Deltaic Estuary. *Photonirvachak: Journal of the Indian Society of Remote Sensing*, 34(4): 431-435.

Gastrell, J.E. 1868. *Geographical and Statistical Report of the Districts of Jessore, Fureedpore and Backergunge*. Office of Superintendant of Govt. Printing, Calcutta: 46p.

Ghosh, A., Schmidt, S., Fickert, F., Nüsser, M. 2015. The Indian Sundarban Mangrove Forests: History, Utilization, Conservation Strategies and Local Perception. *Diversity*, 7: 149–169.

Goodbred Jr., S.L. 2003. Response of the Ganges dispersal system to climate change: A source-to-sink view since the last interstade. *Sedimentary Geology*, 162: 83–104.

Goodbred Jr., S.L., Saito, Y. 2012. Tide-Dominated Deltas. In Davis, R.A., Dalrymple, R.W. (editors. *Principles of Tidal Sedimentology*, Springer Science+Business Media, Dordrecht: 129–149.

Goodbred Jr., S.L., Kuehl, S.A. 2000a. The significance of large sediment supply, active tectonism, and eustasy on margin sequence development: Late Quaternary stratigraphy and evolution of the Ganges-Brahmaputra delta. S*edimentary Geology*, 133(3-4): 227–248.

Goodbred Jr., S.L., Kuehl, S.A. 2000b. Enormous Ganges–Brahmaputra sediment load during strengthened Early Holocene monsoon. *Geology*, 28(12): 1083–1086.

Goodbred Jr., S.L., Paolo, P.M., Ullah, S.M., Pate, R.D., Khan, S.R, Kuehl, S.A., Singh, S.K., Rahaman, W. 2014. Piecing together the Ganges-Brahmaputra-Meghna River delta: Use of sediment provenance to reconstruct the history and interaction of multiple fluvial systems during Holocene delta evolution. *Geological Society of America Bulletin*, 126(11/12): 1495–1510.

Goswami, A.B., Chakrabarti, P. 1987. Evolution of the Quaternary coastal lowlands of West Bengal, India (Abstract), *Proceeding International Symposium of Coastal Lowlands Geology and Geotectonics*, Den Hague: 117.

Gupta, H.P. 1981. Palaeoenvironment during Holocene time in Bengal Basin, India, as reflected by palynostratigraphy. *Palaeobotanist*, 27(2): 136–160.

Hait, A.K., Das, H., Ghosh, S., Ray, A.K., Saha, A.K., Chanda, S. 1996. New dates of Pleisto-Holocene subcrop samples from south Bengal, India. *Indian Journal of Earth Sciences*, 23(1-2): 79–82.

Hanebuth, T.J.J., Kudrass, H.R., Linstadter, J., Islam, B., Zander, A.M. 2013. Rapid coastal subsidence in the central Ganges–Brahmaputra Delta (Bangladesh) since the 17th century deduced from submerged salt-producing kilns. *Geology*, 41(9): 987–990.

Haque, M., Alam, M. 1997. Subsidence in the Lower Deltaic area of Bangladesh. *Marine Geodesy*, 20(1): 105–120.

Hazra, S., Ghosh, T., Dasgupta, R., Sen, G. 2002. Sea level and associated changes in Sundarbans. *Science and Culture*, 68(9-12): 309–321

Heroy, D.C., Kuehl, S.A., Goodbred Jr., S.L. 2003. Mineralogy of the Ganges and Brahmaputra rivers. implications for river switching and Late Quaternary climate change, *Sedimentary Geology*. 155: 343–359

Hirst, F.C. 1915. *Report on the Nadia Rivers*. Reprinted in: *Rivers of Bengal: A Compilation*. 2002 reprint. 3(1), West Bengal District Gazetteers, Government. of West Bengal, Kolkata: 1–183.

Hirst, F.C., 1917. *The Surveys of Bengal by Major James Rennell: 1764-1777 (Illustrated by a New Atlas Containing Important Unpublished Maps by Rennell)*. The Bengal Secretariat Book Depot, Calcutta: 51 p.

Hossain, M.S., Uddin, M.J., Fakhuruddin, A.N.M. 2013. Impacts of shrimp farming on the coastal environment of Bangladesh and approach for management. *Reviews in Environmental Science and Bio/Technology*, 12: 313–332.

Hunter, W.W. 1875. *A Statistical Account of Bengal*, 1 (Districts of 24 Parganas and Sundarbans), Trubner and Co., London: 404p.

IMD: India Meteorological Department. 1983. *Climatological Tables of Observatories in India (1931-1960)*, reprinted, Pune: 41–42.

IMD: India Meteorological Department. 2010. *Severe Cyclonic Storm Aila: A Preliminary Report*. Regional Specialised Meteorological Centre, New Delhi: Retrieved on 2010-06-07 from: <www.imd.gov.in/section/nhac/dynamic/aila.pdf>.

IMD: India Meteorological Department. 2012. *Cyclone eAtlas: Electronic Atlas of Tracks of Cyclones and Depressions in the Bay of Bengal and Arabian Sea 1891–2007)* ver-1.0. with updates up to 2015 from <http://www.rmcchennaieatlas.tn.nic.in>.

IPCC: Intergovernmental Panel on Climate Change. 2013. *Climate Change 2013: The Physical Science Basis.* Contribution of Working Group I to the 5th Assessment Report, Cambridge University Press, Cambridge: 1535p.

Islam, M.S. 2001. *Sea-Level Changes in Bangladesh: The Last Ten Thousand Years*. Asiatic Society of Bangladesh, Dhaka: 185p.

Jack, J.C. 1918. *Bengal District Gazetteers: Bakarganj*. Bengal Secretariat Book Depot, Calcutta: 175p.

Khan, A.A. 1991. Tectonics of the Bengal basin. *Journal of Himalayan Geology*, 2(1): 91–101

Kuehl, S., Levy, B.M., Moore, W.S., Allison, M.A. 1997. Subaqueous delta of the Ganges-Brahmaputra river system. *Marine Geology*, 144: 81–96

Kuehl, S.A., Allison, M.A., Goodbred, S.L., Kudrass, H. 2005. The Ganges–Brahmaputra delta. In: Giosan, L., Bhattacharya, J. (editors): *River Deltas—Concepts, Models, and Examples*. SEPM Special Publication, 83: 413–434.

Kuehl, S.A., Hariu, T.M., Moore, W.S. 1989. Shelf sedimentation off the Ganges-Brahmaputra river system: Evidence for sediment bypassing to the Bengal fan. *Geology*, I7(12): 1132–1135.

Lawver, L.A., Scalter, J.G., Meinke, L. 1985. Mesozoic and Cenozoic reconstructions of the south Atlantic. *Tectonophysics*, 114: 233–254.

Lee T.Y., Lawver L.A. 1995. Cenozoic plate reconstruction of southeast Asia. *Tectonophysics*, 251: 85–138.

Milliman, J.D., Syvitski, J.P.M. 1992. Geomorphic/tectonic control of sediment discharge to the ocean: The importance of small mountainous rivers. *Journal of Geology*, 100(5): 525–544.

Mörner, N.-A. 2010a. Some problems in the reconstruction of mean sea level and its changes with time. *Quaternary International*, 221: 3–8.

Mörner, N.-A. 2010b. Sea level changes in Bangladesh new observational facts. *Energy & Environment*, 21(3): 235–249.

Mukherjee, K.N. 1969. Nature and problems of neo-reclamation in Sundarbans. *Geographical Review of India*, 31(4): 1–9.

Mukherjee, K.N. 1976. Harmonious solution of the basic problem of Sundarban reclamation, *Geographical Review of India*, 38(3): 311–315.

Nandy, D.R. 1986. Tectonics, seismicity and gravity of north-western India and adjoining region. *Geology of Nagaland Ophiolites, Memoirs of the Geological Survey of India*, 119: 13–17.

Nandy, D.R. 2001. *Geodynamics of Northeastern India and the Adjoining Region*. ACB Publications, Kolkata: 209p.

Nandy, S., Bandyopadhyay, S. 2010. Trend of sea level change in the Hugli estuary, India. *Indian Journal of Geo-Marine Science*, 40(6): 802–812.

Niyogi, D. 1972. Quaternary mapping in plains of West Bengal, *Proceeding Seminar on Geomorphology, Geohydrology and Geotechtonic of the Lower Ganga Basin*, Indian Institute of Technology, Kharagpur: A71–A80.

Niyogi, D. 1975. Quaternary geology of the coastal plain in the West Bengal and Orissa, *Indian Journal of Earth Science*, 2(1): 51–61.

Pargiter, F.E. 1934. *A Revenue History of the Sundarbans from 1765 to 1870*. 2002 reprint. West Bengal District Gazetteers, Government of West Bengal, Kolkata: 415p.

Pethick, J. 1984. *An Introduction to Coastal Geomorphology*. Edward Arnold, London: 259p.

Pethick, J. 1994. Estuaries and wetlands: Function and form. In Falconer, R.A., Goodwin P. (editors): *Wetland Management*. Thomas Telford, London: 75–142.

Pethick, J., Orford, J.D. 2013. Rapid rise in effective sea-level in southwest Bangladesh: Its causes and contemporary rates. *Global and Planetary Change*, 111: 237–245.

Pirazzoli, P.A. 1996. *Sea Level Changes: The Last* 20000 *Years*, John Wiley and Sons, New York: 211p.

Postma, H. 1967. Sediment transport and sedimentation in the marine environment. In Lauff, G.H. (editor): *Estuaries*. American Association for the Advancement of Science Publication 83, American Association for the Advancement of Science, Washington DC: 158–186.

Pugh, D. 2004. *Changing Sea Levels: Effects of Tides, Weather and Climate*, Cambridge University Press, Cambridge: 265p.

Raha, A.K., Mishra, A., Bhattacharya, S., Ghatak, S., Pramanick, P., Dey, S., Sarkar, I., Jha, C. 2014. Sea Level Rise and Submergence of Sundarban Islands : A Time Series Study of Estuarine Dynamics. *Journal of Ecology and Environmental Sciences*, 5(1): 114–123.

Rahman, A.F., Dragoni, D., El-Masri, B. 2011. Response of the Sundarbans coastline to sea level rise and decreased sediment flow: A remote sensing assessment. *Remote Sensing of Environment*, 115: 3121–3128.

Rahman, M.M. 2012. Time-series analysis of coastal erosion in the Sundarbans mangroves. *International Archives of the Photogrammetry, Remote Sensing and Spatial Information Sciences* (22nd ISPRS Congress, Melbourne) 39(B8): 425–429.

Reading, H.G., Collinson, J.D. 1996. Clastic Coasts, In Reading H.G. (editor): *Sedimentary Environments: Processes, Facies and Stratigraphy*, 3rd edition, Blackwell Science Ltd. Oxford: pp 154–231.

Reaks, H.G. 1919. Report on the physical and hydraulic characteristics of the delta. In Stevenson-Moore, C.J., Ryder, C.H.D., Nandi, M.C., Law, R.C., Hayden, H.H., Campbell, J., Murray, Stevenson-Moore, C.J., Ryder, C.H.D., Nandi, M.C., Law, R.C., Hayden, H.H., Campbell, J., Murray, A. R., Addams-Williums, C., Constable, E.A., *Report on the Hooghly River and its Headwaters*. 1, Bengal Secretariat Book Depot, Calcutta: 29–132. Maps in vol. 2.

Reitz, M.D., Pickering, J.L., Goodbred Jr., S.L., Paola, C., Steckler, M.S., Seeber, L., Akhter, S.H. 2015. Effects of tectonic deformation and sea level on river path selection: Theory and application to the Ganges-Brahmaputra-Meghna River Delta, *Journal of Geophysical Research: Earth Surface*, 120, 671–689.

Rennell, J. 1778. An account of the Ganges and Burampooter rivers, *Philosophical Transactions*. Reprinted as an appendix to Rennell, J. (1788): *Memoir of a Map of Hindoostan or the Mogul Empire*, M. Brown, London: 251–258.

Rennell, J. 1779. *A Bengal Atlas: Containing Maps of the Theatre of War and Commerce on that side of Hindoostan*. Map #2.

Richards, J.F., Flint, E.P. 1990. Long-term transformations in Sundarbans wetlands forests of Bengal. *Agriculture and Human Values*. 7(2): 17–34.

Rogers, K.G., Goodbred, S.L., Mondal, D. 2013. Monsoon Sedimentation on the "abandoned" tide-influenced Ganges-Brahmaputra Delta plain. *Estuarine Coastal and Shelf Science*, 131: 297–309.

Sarwar, M.G., Woodroffe, C.D. 2013. Rates of shoreline change along the coast of Bangladesh. *Journal of Coastal Conservation*, 17(3): 515–526.

Sarwar, M.G.B. 2013. Sea-Level Rise along the Coast of Bangladesh. In Shaw, R., Mallick, F., Islam, A. (editors): *Disaster Risk Reduction Approaches in Bangladesh*, Springer Japan: 217–231.

Saxena, I.P., Singh, C.K., Kumar, S. 1982. Palaeoenvironment analysis of Post-Eocene sequence, Bengal Basin. *Petroleum Asia Journal*, 7(1): 26–32.

Sen, P. K., Banerjee, M. 1990. Palyno-plankton stratigraphy and environmental changes during the Holocene in the Bengal basin, India. In Truswell, E.M., Owen, J.A. (editors). *Proceedings, 7th International Palynological Congress*, 2, *Review Palaeobotany Palynology*, 65(1): 25–35.

Sengupta, R., Murty, C.S., Bhattathiri, P.M.A. 1989. The environmental characteristics of the Hugli estuary. In Bose, A.N., Dwivedi, S.N., Mukhopadhyay, D., Danda, A.K., Bandyopadhyay, K.K. (editors): *Coast Zone Management of West Bengal*, Sea Explorers' Institute, Calcutta: E19–E56.

Sherwill, W.S. 1858. Report on the Rivers of Bengal and Papers of 1856, 1857 and 1858 on the Damoodah Embankments etc., In *Selections from the Records of the Bengal Government*, 29, G. A. Savielle Printing and Pub. Co. (Ltd.), Calcutta: 1–18.

Sneadaker, S.C. 1982. Mangrove species zonation: Why? In Sen, D.N., Rajpurohit, K.S. (editors): *Tasks for Vegetation Science*, W. Jank, the Hague: 111–125.

SoI: Survey of India 2015. *Tide Tables for the Hugli River 2016*. Government of India, Dehradun: 176p.

Stanley, D.J., Hait, A.K. 2000. Holocene Depositional Patterns, Neotectonics and Sundarban Mangroves in the Western Ganges-Brahmaputra Delta. *Journal of Coastal Research*, 16(1): 26–39.

Steckler, M.S., Akhter, S.H., Seeber, L. 2008. Collision of the Ganges–Brahmaputra Delta with the Burma Arc: Implications for earthquake hazard. *Earth and Planetary Science Letters*, 273: 367–378.

Thom, B.G. 1984. Coastal landforms and geomorphic processes. In Sneadaker, S.C., Sneadaker, J.G. (editors): *The Mangrove Ecosystem: Research Methods*, UNESCO, Paris: 3–17.

Tomlinson, P.B. 1986. *The Botany of Mangroves*, Cambridge University Press, Cambridge: 418p.

Umitsu, M. 1987. Late Quaternary sedimentary environments and landforms evolutions in the Bengal lowlands. *Geographical Review of Japan*, B60(2): 164–178.

Umitsu, M. 1993. Late quaternary sedimentary environments and landforms in the Ganges Delta. In Woodroffe, C.D. (editor): *Late Quaternary Evolution of Coastal and Lowlands Riverine Plains of Southeast Asia and Northern Australia*, *Sedimentary Geology*, 83: 177–186.

Untawale, A.G., Jagtap, T.G. 1991. Floristic composition of the deltaic regions of India. In Vaidyanadhan, R. (editor): *Quaternary Deltas of India*, *Memoir Geological Society of India*, 22: 243–263.

UoH-SLC: University of Hawaii - Sea Level Center. 2015. *Research Quality Hourly Tide Gauge Data*. Retrieved on 2016-05-01 from <http://uhslc.soest.hawaii.edu/data/?rq>.

Walker, J. M. 1983. The ocean–atmosphere system. In Couper, A. (editor): *The Times Atlas of the Oceans*, Times Book Ltd., London: 44–67.

Warrick R., Oerlemans, J. 1990. Sea level rise In Houghton, J.T., Jenkins, G.J., Epharaums, J.J. (editors): *Climate Change—The IPCC Scientific Assessment*, Cambridge University Press, Cambridge: 257–281

Wasson, R.A. 2003. A sediment budget for the Ganga–Brahmaputra catchment. *Current Science*, 84: 1041–1047.

Webster, P.J., Holland, H.J., Curry, H.R., Chang, R. 2005. Changes in tropical cyclone number, duration, and intensity in a warming environment. *Science*. 309: 1844–1846.

Wright, L.D. Coleman, J.M., Thom, B.G. 1973. Processes of channel development in a high-tide-range environment: Cambridge Gulf-Ord river delta, western Australia. *Journal of Geology*, 81(1): 15–41.

TABLE CAPTIONS

Table 1: Sedimentation phases in Bengal basin (based on Alam *et al*., 2003)

Table 2: Selected estimates of Holocene sea level and rates of rise in the GBD

Table 3: Summary of stratigraphic facies of the Ganga-Brahmaputra delta (after Goodbred and Kuehl, 2000a)

Table 4: Generalised classification of landforms in the islands of Sundarban

Table 5: Trends of relative mean sea level from tidal observatories of the coastal GBD in the vicinity of the Sundarban

Table 6: Sediment budget of the Sundarban forests (Source: Rogers *et al*., 2013)

FIGURE CAPTIONS

Figure 1: Physiographic setting of the Ganga Brahmaputra delta. The plateaus and other highlands generally occupy the zones above 60 m. Elevation of the alluvial fans, palaeodeltas and Pleistocene terraces approximately range between 25 and 60 m. Areas lower than this form the delta proper. The elevations of the delta roughly decrease from NW to SE. Gradient- and process-based divisions of the delta adapted from Wilson and Goodbred (2015). Limit of the Sundarban region shown in yellow dashed line; see Fig. 9 for details of this boundary. CTFB stands for Chittagong–Tripura Fold Belt. Elevation model prepared from 90-m Shuttle Radar Topography Mission data of 2000

Figure 2: Palaeographic reconstructions showing the position of the Bengal basin region (A) at the break-up of the Gondwanaland in Early Cretaceous; (B) in a continental shelf-slope setting in the northward drifting island-continent of India in Mid-Palaeocene and (C) in Early Miocene prior to acquiring its eastern boundary in form of the Indo-Burman and associated ranges. 'BB' stands for the Bengal basin region, shown in red. Blue indicates oceans and other colours represent continents. Undifferentiated areas are shown in white. The area termed Greater India was consumed in the subduction process and crustal shortening during formation of the Himalaya. *Source*: based on Alam *et al*.'s (2003) adaptation of Lee and Lawver (1995). Drift velocities from Lee and Lawver (1995)

Figure 3A: The Bengal basin and its surroundings featuring the chief tectonic elements. The Hinge Zone marks the outer edge of the continental shelf of the Indian craton and initiation of southeastward attenuation of the continental crust (Tectonic Province-1). The Barisal-Chandpur Gravity High marks the transition from continental to oceanic crust at the base of the Bengal basin (Tectonic Province-2). CTFB and CCF stand for Chittagong–Tripura Fold Belt (Tectonic Province-3) and Chittagong–Cox's Bazar Fault respectively. CCF is the approximate linearity along which the Indian Plate is now subducting beneath the Burma platelet. Red triangles denote Tertiary volcanic centres, formed out of the ongoing subduction. *Source*: after Alam *et al*. (2003). Some Elements are incorporated from Nandy (2001) and Gani and Alam (2003)

Figure 3B: West–East section across the Bengal basin showing major tectonic and crustal features. Volcanics are shown in red. See Fig. 3A for location of the section line. *Source*: after Alam *et al*. (2003)

Figure 4: Plot of ^{14}C dates against depth of organic samples from the Ganga-Brahmaputra delta. Subsidence and tectonic instability is a major concern for accuracy and standardisation of results. Plots joined by a line come from same borehole. The

Younger Dryas represents a brief cold period between c. 12.7 and 11.5 ka BP. *Source*: after Goodbred and Kuehl (2000a) with data of Islam (2001) incorporated

Figure 5: Panels representing principal features of the Late Quaternary evolution of the Ganga–Brahmaputra delta. See text for explanation. Br, Md and SNG stand for the Barind tract, Madhupur terrace and Swatch of No Ground submarine canyon respectively. Cf: Fig. 6. *Source*: modified after Goodbred and Kuehl (2000a)

Figure 6: Schematic section showing sequence stratigraphy of the Holocene Ganga–Brahmaputra delta (vertical exaggeration: 1000×). Transgressive facies belong to on-lapping sequences and high-stand regressive facies to off-lapping formations. Other elements of the diagram are explained in the text. SNG stands for Swatch of No Ground submarine canyon that works as a trap of delta sediments and a conduit of sediment transfer to the deep sea Bengal fan. *Source*: from Goodbred and Kuehl (2000a)

Figure 7: Phases of late Holocene growth of the delta, associated with progressive shifts of the Ganga (G1, G2 & G3), Brahmaputra (B2 & B2) and combined Ganga–Brahmaputra (GB-1) discharges as suggested by Allison *et al*. (2003). Major morphological features of the GBD are also shown. The Barind tract and Madhupur terrace are uplifted blocks with remnant Pleistocene surfaces that separate the delta into different compartments and hinder free swinging of rivers across the delta. Morphostratigraphically equivalent formations are seen in the palaeodeltaic surfaces bordering the Chhotanagpur plateau. The hinge zone is a flexure of the subsurface continental shelf to the deeper basin areas. Reddish tinge in the coastal region denotes the Sundarban mangroves. See Fig. 1 for altitudinal reference. False Colour Composite prepared from IRS-1D WiFS data of 3 March 1998. *Source*: from Bandyopadhyay (2007)

Figure 8: Stages of biotidal accretion in a tropical delta. The process starts from colonisation of grasses, herbs and shrubs that help to stabilise intertidal shoals. With rise in elevation, interval of tidal inundation reduces, and leads to successive changes in mangrove species. At maturity, the shoal evolves into a supratidal island with non-mangrove climax vegetation that is inundated only during episodic storm surges. *Source*: after Untawale and Jagtap (1991)

Figure 9: Composite map of the Sundarban. 1829-30 extent of the mangrove wetlands is indicated by the Dampier–Hodges (D–H) Line that is still regarded as the northern limit of the Sundarban region in India. In Bangladesh, Sundarban refers to the forests only, with its impact area demarcated by two buffers. Comparison between 1901–23 topographical maps and 2013–15 satellite images brings out the extent of erosion along nearly the entire seaface of the delta and accretion in the interior parts, mainly in the west. Tide stations referred to in Fig. 10 are also shown in the map as are selected populated places. *Source*: coastline and channel banks extracted from 37 mosaiced Survey of India 1:63,360 topographical maps of 1901–23, belonging to 79B, C, F & G series; Landsat 8 OLI 15-m panfused data of 17 Mar 2015 & 8 Mar 2015 (for Bangladesh part); IRS-R2 LISS-4fx 5.6-m data of 23 Feb 2013 & 1 Jan 2014 (for India part). D–H Line extracted from 1:253,440 Atlas of India map # 121 & 122 of c. 1860

Figure 10: Tidal characteristics of the lower GBD at or close to the Sundarban region. (**A**) Landward amplification of tidal range (n=26). Sagar, Gangra, Haldia, and Diamond Harbour are situated along the Hugli estuary. Hiron Point, Sundarikota, and Mongla are situated along the Pussur, where the tidal range is comparatively lower. *Source*: SoI, 2015 (Hugli estuary stations); Chatterjee *et al.*, 2013 (Indian Sundarban stations); BIWTA, 2015 (Bangladesh stations). (**B**) Landward enhancement of tidal

asymmetry (n=24). All stations shown in (A) are not represented due to non-availability of data. See Fig. 9 for location of stations. *Source*: SoI, 2015 (Hugli estuary stations); Chatterjee *et al*., 2013 (Indian Sundarban stations); UoH-SLC, 2015 and BIWTA, 2016 (Bangladesh stations)

Figure 11: Tropical cyclones landfalling in the Sundarban region between 88° and 90° E. Trends indicate that a future rise in frequency in probably imminent. Depression: a storm with 10-min average wind speed of 31–61 km h^{-1}; Cyclonic Storm: 62–88 km h^{-1}; Severe Cyclonic Storm: >89 km h^{-1}. *Source*: <http://www.rmcchennaieatlas.tn.nic.in>

Figure 12: Available RMSL trends (in mm a–1) in the coastal Ganga–Brahmaputra delta at or close to the Sundarban region. Data of Khepupara and Sagar are not represented by bars because of their anomalous values. Blue and magenta dotted lines denote the limits of the Sundarban Blocks in India and Sundarban Impact Zone in Bangladesh, respectively; black line is the international boundary. *Source*: see Table 5

Figure 13: Coastal retreat in the Sundarban is highest between the Saptamukhi and the Hariabhanga estuaries. Here the Bulchery is represented to show relentlessness of the erosion through different years. Like other sea-facing islands of the area, its area reduced by 50% within the last 100 a and is likely to get obliterated within the next 100 a or so. *Source*: 1922-23 & 1942: SoI 'inch' topomaps #76C/06 on 1:63,336 (two editions); 1968-69: SoI 'metric' topomap #76C/06 on 1:50,000; 2001: IRS-1D LISS-3+Pan 5.6-m data of January 2001; 2013 (base image): IRS-R2 LISS-4fx 5.6-m data of 23 Feb 2013.

Figure 14: Transformation of tidal creeks into water bodies in Satjaliya island (coded Gb-06) of Gosaba block of western Sundarban from 1920-21 (A) through 1968-69 (C) and 2001 (D). The changes are compared in the bottom left diagram. In 1920-21, when the island was under forests, there were hardly any water bodies in the island. During its subsequent reclamation, a number of tidal creeks were blocked at their entrances and a marginal embankment was constructed all around the island and along the major channels. This transformed the free-flowing water courses to stagnant water bodies. With time, these water bodies were subjected to eutrophication and/or land-filling for expansion of farmlands or for habitational use. In contrast, none of the creeks in the adjacent non-reclaimed areas lost their original density. *Source*: (A) SoI 'inch' Map # 79B/16 on 1:63,360; (B) SoI 'metric' Map # 79B/16 on 1:50,000; (C) IRS-1D LISS-L3+Pan data of January 2001

Figure 15: Position of the Swatch of No Ground canyon in the continental shelf of the Ganga-Brahmaputra delta. The swatch bisects the shelf region into two and acts as a conduit for interception and transport of sediments to the deep sea Bengal fan (red arrows). This may have augmented the retreat of the coastline in the fluvially abandoned Sundarban region. However, interior parts of the Sundarban are getting actively vertically accreted by tidal reworking of sediments (green arrows). *Source*: isobaths from National Hydrographic Office Chart No. 31